https://pubsonline.informs.org/journal/ijoc

INFORMS JOURNAL ON COMPUTING
Vol. 36, No. 1, January–February 2024, pp. 39–60
ISSN 1091-9856 (print), ISSN 1526-5528 (online)

Detecting Critical Nodes in Sparse Graphs via "Reduce-Solve-Combine" Memetic Search

Yangming Zhou,[a,b] **Jiaqi Li,**[c] **Jin-Kao Hao,**[d,*] **Fred Glover**[e,*]

[a] Sino-US Global Logistics Institute, Antai College of Economics and Management, Shanghai Jiao Tong University, Shanghai 200030, China; [b] Data-Driven Management Decision Making Lab, Shanghai Jiao Tong University, Shanghai 200030, China; [c] Department of Computer Science and Engineering, East China University of Science and Technology, Shanghai 200237, China; [d] LERIA, Université d'Angers, Angers 49045, France; [e] Entanglement, Inc., Boulder, Colorado 80302

*Corresponding author

Contact: yangming.zhou@sjtu.edu.cn, https://orcid.org/0000-0002-4254-6517 (YZ); y30211039@mail.ecust.edu.cn, https://orcid.org/0000-0001-8641-9969 (JL); jin-kao.hao@univ-angers.fr, https://orcid.org/0000-0001-8813-4377 (J-KH); fred@entanglement.ai, https://orcid.org/0000-0001-6945-0438 (FG)

Received: April 29, 2022
Revised: December 20, 2022; April 27, 2023; July 10, 2023
Accepted: July 14, 2023
Published Online in Articles in Advance: August 23, 2023

https://doi.org/10.1287/ijoc.2022.0130

Abstract. This study considers a well-known critical node detection problem that aims to minimize a pairwise connectivity measure of an undirected graph via the removal of a subset of nodes (referred to as critical nodes) subject to a cardinality constraint. Potential applications include epidemic control, emergency response, vulnerability assessment, carbon emission monitoring, network security, and drug design. To solve the problem, we present a "reduce-solve-combine" memetic search approach that integrates a problem reduction mechanism into the popular population-based memetic algorithm framework. At each generation, a common pattern mined from two parent solutions is first used to reduce the given problem instance, then the reduced instance is solved by a component-based hybrid neighborhood search that effectively combines an articulation point impact strategy and a node weighting strategy, and finally an offspring solution is produced by combining the mined common pattern and the solution of the reduced instance. Extensive evaluations on 42 real-world and synthetic benchmark instances show the efficacy of the proposed method, which discovers nine new upper bounds and significantly outperforms the current state-of-the-art algorithms. Investigation of key algorithmic modules additionally discloses the importance of the proposed ideas and strategies. Finally, we demonstrate the generality of the proposed method via its adaptation to solve the node-weighted critical node problem.

History: Accepted by Erwin Pesch, Area Editor for Heuristic Search & Approximation Algorithms.
Funding: This work was supported by the National Natural Science Foundation of China [Grants 72371157, 61903144, 72031007].
Supplemental Material: The software that supports the findings of this study is available within the paper and its Supplemental Information (https://pubsonline.informs.org/doi/suppl/10.1287/ijoc.2022.0130) as well as from the IJOC GitHub software repository (https://github.com/INFORMSJoC/2022.0130). The complete IJOC Software and Data Repository is available at https://informsjoc.github.io/.

Keywords: critical node problem • memetic search • instance reduction • reduce-solve-combine • heuristic search

1. Introduction

Given an undirected graph $G = (V, E)$ with vertex (or node) set V and edge set E, critical node detection problems (CNDPs) (Arulselvan et al. 2009, Naoum-Sawaya and Buchheim 2016, Zhou et al. 2019, Baggio et al. 2021, Zhou et al. 2021b, Salemi and Buchanan 2022) aim to identify a subset of nodes (referred to as *critical nodes*) $S \subseteq V$ whose removal enhances (decreases) the graph connectivity of the residual graph $G[V \setminus S]$ evaluated by a given connectivity measure σ. According to different cases of $|S|$ and σ, CNDPs can be divided into two categories: K-vertex-CNDP and β-connectivity-CNDP. The former is to optimize (minimize or maximize) the connectivity measure σ, such that no more than K nodes are deleted (i.e., $|S| \leq K$), whereas the latter aims to minimize the set of deleted nodes, such that the connectivity measure σ is bounded by a given threshold β (Zhou et al. 2023d). A detailed taxonomy of CNDPs is provided in (Zhou et al. 2021b). In addition, node-weighted CNDPs (Chen et al. 2020, Zhou et al. 2021c) and distance-based CNDPs (Salemi and Buchanan 2022, Zhou et al. 2023c) have been receiving increasing attention in the literature.

The critical node problem (CNP) (Arulselvan et al. 2009, Zhou et al. 2019, Baggio et al. 2021) is a fundamental CNDP, which belongs to the category of K-vertex-CNDPs. It seeks a set $S \subseteq V$ of at most K nodes, the deletion of which minimizes the total pairwise connectivity in $G[V \setminus S]$. Formally, the objective function $f(S)$ of CNP can be written as follows:

$$f(S) = \sum_{i=1}^{M} \frac{|\mathcal{C}_i|(|\mathcal{C}_i| - 1)}{2}, \tag{1}$$

where $\mathcal{C}_i$ is a connected component, and M is the total number of connected components in the residual graph $G[V \setminus S]$. Hence, the residual graph $G[V \setminus S]$ is composed of M connected components, that is, $\sum_{i=1}^{M} \cup \mathcal{C}_i = G[V \setminus S]$. From (1), we observe that a good solution of CNP should generate a residual graph that maximizes the number of connected components while simultaneously minimizing the variance in the component sizes.

CNP has a wide spectrum of applications in many fields. For example, the overall transmissibility of a virus can be limited by identifying only a specific number of people to be vaccinated in epidemic control (Doostmohammadian et al. 2020). Emergency response can be modeled as a CNP by identifying some critical nodes that can be used to plan good emergency evacuations at a disaster case (Vitoriano et al. 2011). Besides epidemic control and emergency response, CNP is also a convenient model for other applications such as vulnerability assessment (Nguyen et al. 2013, Zhou et al. 2021c), carbon emission monitoring (Zhang et al. 2020), network security (Mugisha and Zhou 2016), and drug design (Abbas et al. 2021).

CNP is known to be NP-hard on general graphs (Arulselvan et al. 2009). Its solution space grows exponentially with its size. As indicated in (Veremyev et al. 2014a), CNP can be solved exactly on medium sparse graphs with up to 1,500 nodes under the time limit 50,000 seconds. However, CNP instances from real-world applications can be considerably larger. To deal with such instances, computationally efficient heuristic algorithms have been developed to provide high-quality solutions in reasonable computation time. To the best of our knowledge, two population-based memetic algorithms with fixed or variable population represent the current state-of-the-art for solving CNP (Zhou et al. 2019, 2021b). However, these algorithms are time-consuming, which becomes a handicap when they are applied on large graphs. This motivates us to incorporate a strategy based on the divide-and-conquer principle that divides an original problem into several subproblems to solve them separately, followed by combining the solutions of the subproblems to yield an overall solution of the original problem. To take advantage of both the memetic search framework and the divide-and-conquer principle, this work introduces a "reduce-solve-combine" (RSC) memetic algorithm that integrates a problem reduction mechanism into the popular memetic algorithm framework.

The main contributions of the work are summarized as follows:

- The proposed algorithm, called instance reduction-based memetic search (IRMS), incorporates an RSC mechanism within the popular population-based memetic algorithm framework. At each generation, a common pattern mined from two parent solutions is first used to reduce the original instance, then the reduced instance is solved, and an offspring solution is finally obtained by combining the mined common pattern and the solution of the reduced instance. In addition, a component-based hybrid neighborhood search that combines the articulation point impact and node weighting strategies is developed to ensure an effective local optimization. It is worth noting that the reduced instance can be approximately solved by a heuristic solver or optimally solved by an exact solver in the RSC module. Moreover, this module is of a generic nature, which can be combined with other heuristic algorithms to improve their search performances.
- The proposed IRMS algorithm achieves a high level of performance on the 42 synthetic and real-world benchmark instances commonly used in the literature that compares very favorably with the state-of-the-art CNP algorithms, finding new upper bounds for 9 instances. Our experimental results also disclose the superiority of IRMS over the most recent frequent pattern-based search (FPBS) (Zhou et al. 2022), which is based on mining patterns from a set of high-quality solutions with a time-consuming frequent itemset mining algorithm to guide the offspring solution construction. Experimental analyses on key algorithmic modules of the proposed algorithm are performed to identify the elements underlying the effectiveness of the proposed ideas and techniques.
- We also demonstrate the inherent generality of the proposed IRMS algorithm by an application to solve the node-weighted critical node problem, where this generalized version of IRMS performs significantly better than the best-performing algorithm for the node-weighted problem in terms of both the best and average values.

The rest of this paper is organized as follows. After a brief review of previous studies on CNP and instance reduction techniques in Section 2, we present IRMS for CNP in Section 3. Section 4 conducts experimental studies of the proposed algorithm and compares its results with those of the state-of-the-art methods. The generalization of IRMS that adapts it to the node-weighted CNP is presented in Section 5. Key issues of IRMS are analyzed in Section 6, followed by conclusions in Section 7.

2. Related Work

2.1. Previous Studies on CNP

The CNP has been shown to be NP-hard (Arulselvan et al. 2009) and has attracted widespread research attention (Arulselvan et al. 2009; Pullan 2015; Veremyev et al. 2019; Zhou et al. 2019, 2021b). Existing solution approaches can be divided into two categories: exact and heuristic algorithms. Exact algorithms can theoretically guarantee the optimality of their obtained solutions. For example, Arulselvan et al. (2009) presented the first integer programming model with $O(|V|^2)$ variables and $O(|V|^3)$ constraints for CNP and used CPLEX to solve the model. Di Summa et al. (2012) further proposed two improved formulations: an extended formulation of (Arulselvan et al. 2009) and a quadratic programming reformulation considering the complete form of CNP. Both are solved with the branch-and-cut framework. Because of the large number of constraints (i.e., $O(|V|^3)$), the exact algorithms could solve CNP to optimality only for small sparse graphs with up to 150 nodes. Veremyev et al. (2014b) developed an improved compact linear reformulation with only $O(|V|^2)$ constraints, which was able to provide exact solutions for CNP with up to 1,200 nodes and further developed a general integer programming framework for solving different CNDPs (Veremyev et al. 2014a). Rezaei et al. (2021) proposed an efficient exact iterative algorithm (EIA-CNDP) to solve a CNDP whose objective is to minimize the size of the largest connected component. In addition, they provided a comprehensive survey on both exact and heuristic algorithms for solving different CNDPs.

To deal with large instances, heuristic algorithms are required to solve CNP approximately in an affordable computation time. Existing heuristics for CNP can be grouped into two categories: local search and population-based methods. Local search methods manipulate only a single candidate solution of the given problem in each search step. For example, Arulselvan et al. (2009) presented an early heuristic that starts with an independent set and is coupled with a two-exchange local search. Ventresca (2012) proposed a simulated annealing (SA) algorithm for CNP using a combinatorial unranking-based problem representation. Pullan (2015) developed a multistart greedy algorithm for CNP (CNA1 for short). Addis et al. (2016) proposed several hybrid heuristic algorithms by combining the two basic greedy rules (i.e., add-back and remove) with some flavor of local search. Based on two smart and computationally efficient neighborhoods, Aringhieri et al. (2016b) presented two metaheuristic algorithms for CNP based on the iterated local search (ILS) and variable neighborhood search (VNS) frameworks. More recently, de San Lázaro et al. (2021) proposed an improved VNS algorithm, and Wang and Di (2022) proposed a cluster expansion method called CEMCNP for CNP. CEMCNP uses a strategy similar to that of the multistart ILS algorithm, supplemented by integrating a contraction mechanism to greedily alleviate the effect of vertex scale without loss of accuracy and an incremental cluster expansion approach to iteratively separate the graph into many disconnected components whose sizes are kept within reasonable bounds.

In contrast to the preceding local search methods, population-based methods often maintain a population of candidate solutions that are manipulated and evaluated during the search process. For instance, Ventresca (2012) proposed a population-based method for CNP called the population-based incremental learning (PBIL) algorithm, which used an unranking-based problem representation and obtained higher-quality solutions than SA. However, SA found solutions faster than PBIL. Aringhieri et al. (2016a) designed a general evolutionary algorithm framework for different classes of CNDPs, which followed a simple genetic algorithm framework that made use of greedy rules to repair and correct the solution during the reproduction and mutation phases. Purevsuren et al. (2017) combined a greedy randomized adaptive search procedure (GRASP) with exterior path-relinking for CNP. Following this, Zhou et al. (2019) presented a memetic algorithm for CNP (MACNP for short) and subsequently proposed a variable population memetic search (VPMS) (Zhou et al. 2021b), using a strategic population sizing mechanism to dynamically adjust the population size during the search process. These memetic algorithms adopt a strategy for combining solutions to create new ones similar to that of the path relinking approach (Glover 1997), which invites the relationship between these approaches to be investigated more fully. Unlike the general local search and population-based algorithms, Nabli and Carvalho (2020) proposed a multiagent reinforcement learning framework to learn to solve a multilevel budgeted combinatorial problem. A case study on the multilevel CNP shows this learning algorithms outperforms classical reinforcement learning algorithms.

To the best of our knowledge, most state-of-the-art results of the CNP instances were obtained by memetic algorithms (i.e., MACNP and VPMS), which rely on a fixed or variable population of candidate solutions to explore the search space. However, these algorithms are very time-consuming and have trouble to effectively solve very large instances. It is necessary to propose computationally efficient algorithms capable to deal with such large instances.

2.2. Previous Studies on Instance Reduction

To solve large-scale instances, instance reduction is a useful strategy for a number of difficult combinatorial optimization problems, as shown in various studies in the literature (Zheng and Xue 2010, Wu and Hao 2012, Chen and Hao 2014, Delgadillo et al. 2016, Kenny et al. 2018, de Holanda Maia et al. 2020, Zhang et al. 2021, Le et al. 2022). In the following, we briefly review some representative instance reduction methods fitting different categories.

The divide-and-conquer strategy is a popular and general approach to solve large-scale problems. The main idea is to decompose the original large problem into smaller subproblems that can be solved individually. For the arc routing problem, a commonly used divide-and-conquer strategy is to divide the task into subsets, and then solve the subproblems induced by the task subsets separately. For example, Zhang et al. (2021) proposed a novel problem decomposition operator called the route cutting off operator and integrated it within two state-of-the-art divided-and-conquer algorithms to solve large scale capacitated arc routing problems.

Reduce-and-solve methods represent a closely related derivative of divide-and-conquer approaches illustrated by the work of Zheng and Xue (2010) who use formal calculation rules to divide a discrete optimization problem into subproblems with smaller search spaces and accompanied by efficient implicit algorithms to incrementally construct a complete solution from the solutions to the subproblems. Chen and Hao (2014) developed a reduce-and-solve heuristic approach for the multiple-choice multidimensional knapsack problem, which combined problem reduction techniques with the CPLEX solver. Its basic idea is to use some dedicated heuristics to fix a number of groups and variables to obtain a reduced critical subproblem that is then solved by the CPLEX solver.

Similarly, Wu and Hao (2012) proposed an effective approach called EXTRACOL to coloring large graphs. It first applied a preprocessing procedure to extract large independent sets from the graph, and then used a memetic algorithm to color the residual graph. However, if an independent set extracted in the preprocessing is not part of the optimal coloring, it can never be repaired. To cope with this issue, the authors developed an extraction and expansion method called E2COL, which integrates an expansion phase to allow the coloring process to reconsider each extracted independent set on a one-by-one basis (Wu and Hao 2013). They further extended E2COL by proposing additional strategies, resulting in an improved extraction and expansion algorithm named IE^{2}COL (Hao and Wu 2012), which used a forward independent set extraction strategy to reduce the initial graph, followed by a backward coloring process which uses extracted independent sets as new color classes for intermediate subgraph coloring.

Inspired by the concept of immunization by vaccination derived from artificial immune systems, Montiel et al. (2013) proposed a reduce-optimize-expand method to improve existing discrete optimization algorithms for large-scale traveling salesman problems (TSPs) composed of three steps. The first step decreases the problem complexity by a heuristic for reducing the number of nodes of the original problem. The next step applies an exact or heuristic algorithm to obtain an intermediate solution which is expanded in the third step to produce a final solution. Based on the reduce-optimize-expand method, Delgadillo et al. (2016) presented an intelligent strategy with a fuzzy logic classifier to obtain systematic reductions of TSP instances. In related work, de Holanda Maia et al. (2020) proposed a MineReduce approach to improve a heuristic for the heterogeneous fleet vehicle routing problem by performing problem reductions.

Blum et al. (2016) proposed an alternative hybrid metaheuristic framework called construct, merge, solve, and adapt (CMSA) for combinatorial optimization problems that similarly uses reduced problem instances and works in three phases. First, it generates a reduced subinstance of the original problem instance by a process that ensures a solution to the subinstance is also a solution to the original instance. Second, it applies an exact solver to the reduced subinstance to obtain a high-quality solution of the original instance. Finally, it makes use of the results of the exact solver as feedback for the next algorithm iteration. The method has been successfully applied to solve the minimum common string partition problem and minimum covering arborescence problem.

Kenny et al. (2018) presented a problem reduction metaheuristic called merge search (MS). It consists of three main modules: an initial solution construction heuristic, a SA-based local search to quickly generate a population of neighboring solutions, and a merge operation that uses information from all solutions in the population to produce a reduced subproblem, which is then solved by a mixed integer programming solver. The method has been further extended with an improved population generation and variable aggregation heuristics for the constrained pit problem in (Kenny et al. 2019). The main difference between MS and CMSA is that CMSA generates solutions from scratch, whereas MS starts with a single initial seed solution and uses local search to generate a population of neighboring solutions to the initial seed solution.

Mihic et al. (2018) presented a general-purpose local search approach called randomized decomposition (RD) for solving hard, nonlinear, nonconvex mathematical programs. RD uses a novel decomposition to partition the solution space into random subspaces and then find a local optimum in each subspace independently. In addition to the quadratic assignment problem, the RD decomposition method has been successfully applied to a wide range of

Figure 1. (Color online) Diagram of the Proposed IRMS Approach

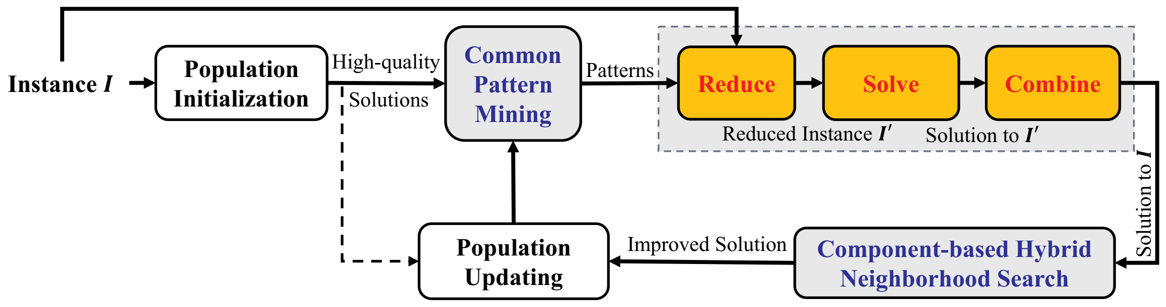

other problems, including revenue management (Cooper and Homem-de-Mello 2007) and traveling salesman problems (Subramanyam and Gounaris 2018).

As mentioned previously, memetic algorithms (i.e., MACNP (Zhou et al. 2019) and VPMS (Zhou et al. 2021b)) are the best performing heuristic algorithms for CNP. In this work, we present an instance reduction-based memetic search (IRMS) approach for CNP, where an RSC instance reduction mechanism is integrated into the well-known memetic algorithm to join the merits of these two strategies for solving large and hard CNP applications.

3. Instance Reduction-Based Memetic Search for CNP

Our instance reduction-based memetic search algorithm for CNP is based on the following key modules.

3.1. Solution Representation and Evaluation

Given a CNP instance with an integer K, any subset $S \subset V$ of size K is a feasible solution, that is, $|S| = K$. A candidate solution S can be represented by $S = \{v_{S(1)}, v_{S(2)}, \dots, v_{S(K)}\}$ such that $S(i)$ is the index of node i in V or equivalently a binary vector of size $|V|$ such that exactly K variables receive the value of one and the other $|V| - K$ variable receives zero. The solution space Ω contains all possible subsets of K nodes, that is, $\Omega = \{S \subset V : |S| = K\}$. The size of Ω is given by $\binom{|V|}{K} = \frac{|V|!}{K!(|V|-K)!}$ and increases rapidly with increases in $|V|$ and K. According to (1), the solution cost of S can be evaluated by a modified depth first search (DFS) algorithm (Hopcroft and Tarjan 1973) in $O(|V| + |E|)$.

3.2. General Scheme

The general scheme of the proposed IRMS approach is illustrated in Figure 1. One distinct feature of IRMS is that a common pattern mined from only two parent solutions is used to guide the instance reduction, and the reduced instance is then solved by a fast local search heuristic. Finally, a promising offspring solution is obtained by directly combining the common pattern and the solution of the reduced instance. From the perspective of algorithm architecture, IRMS is composed of five modules (see Algorithm 1): (1) population Initialization (Section 3.3), (2) component-based hybrid neighborhood search (Section 3.4), (3) common pattern mining (Section 3.5), (4) RSC mechanism (Section 3.6), and (5) population updating (Section 3.7).

The IRMS approach starts with an initial population of λ high-quality solutions (line 1). At each generation, it randomly selects two parent solutions S^F and S^M from the population P (line 4). A common pattern mining procedure is then applied to find a common pattern ζ between S^F and S^M (line 5). An offspring solution S is then generated by the RSC mechanism (line 6), which is further improved by a component-based hybrid neighborhood search (CHNS) procedure (line 7). Finally, a population updating procedure is used to accept or discard the offspring solution (line 11). The process repeats until a given stopping condition is satisfied, such as a time limit $\hat{t}$ or a given number of generations.

Algorithm 1 (Pseudo Code of IRMS Approach for CNP)

```
Input: A CNP instance $I$ (i.e., an undirected graph $G$ with an integer $K$), population size $\lambda$, selection probability
    $\theta$, and maximal idle iteration count $\hat{\xi}$
Output: The best found solution $S^*$
1: $P \leftarrow$ PopulationInitialization($\lambda$)    /* Build an initial population */
2: $S^* \leftarrow \arg\min\{f(S_i) : i = 1, 2, \dots, \lambda\}$    /* Record the best solution $S^*$ */
3: while a stopping condition is not satisfied do
```

```
4:     Randomly select two solutions $S^F$ and $S^M$ from $P$
5:     $\zeta \leftarrow$ CommonPatternMining($S^F, S^M$)    /* Mine common pattern between two parents */
6:     $S \leftarrow$ RSC($I, \zeta$)    /* Construct an offspring solution */
7:     $S' \leftarrow$ CHNS($S, \theta, \hat{\xi}$)    /* Improve the solution */
8:     if $f(S') \le f(S^*)$ then
9:         $S^* \leftarrow S'$
10:    end if
11:    $P \leftarrow$ PopulationUpdating($P, S'$)    /* Update the population */
12: end while
13: return The best found solution $S^*$
```

3.3. Population Initialization

The initial population is composed of λ diverse and high-quality solutions, where each solution is created as follows. A random solution is first generated, which is then improved to a high-quality local optimum by the component-based neighborhood search procedure (Zhou et al. 2019). Then the improved solution is added into the population P if the solution does not duplicate any existing solution in the current population, and the process repeats until λ different high-quality solutions are obtained.

3.4. Component-Based Hybrid Neighborhood Search

3.4.1. Basic Idea. To perform local optimization, we propose a CHNS, which effectively combines the node weighting and articulation point impact strategies. As shown in Algorithm 2, CHNS starts from a candidate solution S, and then iteratively improves it by adding a new node to S (lines 4–11) and greedily removing a node from S (lines 12–13). CHNS stops when the idle iteration count ξ (i.e., the number of iterations without improvement) reaches an allowed maximal value $\hat{\xi}$.

Algorithm 2 (Pseudo Code of CHNS)

```
Input: A solution $S$, selection probability $\theta$, and maximal idle iteration count $\hat{\xi}$
Output: The best solution $S^*$ found
1: $S^* \leftarrow S$
2: $\xi \leftarrow 0$    /* Idle iteration count */
3: while $\xi < \hat{\xi}$ do
4:     Randomly select a large connected component $\mathcal{C}$
5:     Generate a random probability $p \in (0,1)$
6:     if $p < \theta$ then
7:         $v \leftarrow$ ArticulationPointImpact($\mathcal{C}$)    /* Executed with the predefined selection probability $\theta$ */
8:     else
9:         $v \leftarrow$ NodeWeighting($\mathcal{C}$)    /* Executed with the probability $1-\theta$ */
10:    end if
11:    $S \leftarrow S \cup \{v\}$
12:    $u \leftarrow \arg\min\{f(S \setminus \{w\}) - f(S) | w \in S\}$
13:    $S \leftarrow S \setminus \{u\}$
14:    if $f(S) < f(S^*)$ then
15:        $S^* \leftarrow S$
16:        $\xi \leftarrow 0$
17:    else
18:        $\xi \leftarrow \xi + 1$
19:    end if
20: end while
21: return The best solution $S^*$ found
```

Definition 1 (Large Connected Component). A connected component $\mathcal{C}$ is considered as a large connected component if its size is greater than $(\hat{\chi} + \check{\chi})/2$, where $\hat{\chi} = \max_{i\in\{1,\dots,M\}}|\mathcal{C}_i|$ and $\check{\chi} = \min_{i\in\{1,\dots,M\}}|\mathcal{C}_i|$ present the size of largest and smallest connected components in the residual graph $G[V \setminus S]$, respectively.

At each iteration, a large connected component $\mathcal{C}$ is selected randomly. Then, CHNS uses a hybrid node selection strategy to select a node v from $\mathcal{C}$ and combines the node weighting and articulation point impact strategies in a probabilistic way. That is, a node v is selected by the articulation point impact strategy with a selection probability θ $(0 \le \theta \le 1)$, and otherwise is selected by a node weighting strategy as in (Zhou et al. 2019). CHNS can be considered as an improved form of component-based neighborhood search (CBNS) (Zhou et al. 2019) that includes a way to remove a node from a large connected component $\mathcal{C}$ with the articulation point impact strategy described next.

Algorithm 3 (Pseudo Code of Articulation Point Impact Strategy)

```
Input: A large connected component $\mathcal{C}$
Output: The selected node $v^*$
1:  $root \leftarrow$ a random node in $\mathcal{C}$    /* Randomly select a node as the root node */
    //Initialize all arrays
2:  $Count \leftarrow 0$    /* Time stamp */
3:  for all nodes $v \in \mathcal{C}$ do
4:      $dfn[v] = \psi[v] = 0$
5:      $\gamma[v] = \eta[v] = 1$
6:  end for
    //Calculate the impact of each node
7:  TarjanInComponent($\mathcal{C}, root, Count, \gamma, \eta$)
8:  for each node $v \in V_{\mathcal{C}}$ do
9:      if $v$ is an articulation point then
10:         $\psi[v] += \frac{(Count-\eta[v])(Count-\eta[v]-1)}{2}$
11:     else
12:         $\psi[v] += \frac{(Count-1)(Count-2)}{2}$
13:     end if
14:     $v^* \leftarrow \arg\min\{\psi[v] : v \in V_{\mathcal{C}}\}$
15: end for
16: return The selected node $v^*$
```

3.4.2. Articulation Point Impact Strategy. Let $\mathcal{C} = (V_{\mathcal{C}}, E_{\mathcal{C}})$ be a large connected component, where $V_{\mathcal{C}}$ and $E_{\mathcal{C}}$ denote the node set and edge set in $\mathcal{C}$, respectively. The articulation point impact strategy aims to select a node whose removal maximally decreases the connectivity of $\mathcal{C}$ (see Algorithm 3). To quickly find such a node in $\mathcal{C}$, we design a TarjanInComponent procedure based on the algorithm of Tarjan (1972) that traverses every node in a component in only one round with time complexity $O(|V_{\mathcal{C}}| + |E_{\mathcal{C}}|)$ (line 11). The detailed pseudo code of TarjanInComponent is provided in Algorithm 1 of the online supplement (Zhou et al. 2023b). The articulation point impact strategy starts its search from a root of the large connected component $\mathcal{C}$. Any node in $\mathcal{C}$ can be considered as a root node.

A conversion from an original connected component to a DFS tree is illustrated in Figure 2, where Figure 2(a) and (b), respectively, present a connected component of nine nodes and a corresponding DFS tree rooted at node a. As shown in Figure 2(b), black solid arrows indicate tree edges that are taken when visiting unvisited nodes, whereas black dashed arrows denote back edges taken when visiting visited nodes. After removing the node d, the two shaded areas that correspond to two resulting connected components are obtained.

Figure 2. (Color online) An Illustrative Example of a Conversion between (a) an Original Component and (b) the Corresponding DFS Tree

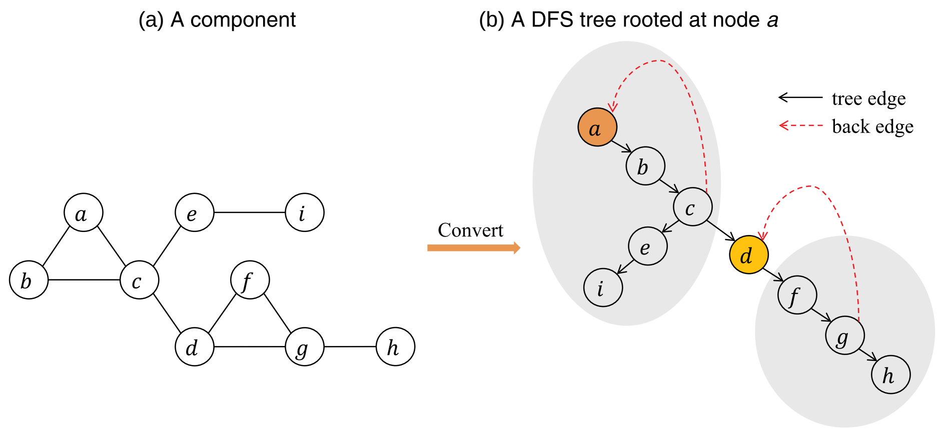

Table 1. Related Parameter Values of the Example Shown in Figure 2

	a	b	c	d	e	f	g	h	i
Time stamp (*dfn*)	1	2	3	6	4	7	8	9	5
Trace value (*low*)	1	1	1	3	3	6	6	8	4
γ	9	8	7	4	2	3	2	1	1
η	1	1	7	4	2	3	2	1	1

Unlike the approach of Ventresca and Aleman (2015), our articulation point impact strategy builds a DFS tree and evaluates its nodes simultaneously. To achieve this, two arrays are defined to record the states of nodes in the tree, that is, time stamps (*dfn*) and trace values (*low*). The former presents the time stamp when a node is first visited (i.e., the traverse sequence number), whereas the latter records the trace value of the node (i.e., the smallest time stamp of the current node's neighbor visited). Therefore, we can obtain *dfn*, *low*, γ, and η values of the previously mentioned example, as summarized in Table 1.

Definition 2 (Articulation Point). An articulation point (or cut vertex) of a graph is a node whose deletion with associated edges makes the original graph disconnected, or more precisely, increases the number of connected components in the graph.

From a DFS tree, we have two simple observations.

Remark 1. A leaf node is not an articulation point.

Remark 2. A root node with at least two subtrees is an articulation point.

Suppose u is an internal node (i.e., neither a leaf node nor a root node), v is an arbitrary node, and $e(u,v)$ is the edge between nodes u and v. We calculate *low* values according to the following rules:

- If $e(u,v)$ is a tree edge of the graph, then we have $low[u] = \min\{low[u], low[v]\}$;
- If $e(u,v)$ is a back edge of the graph and v is not the parent of u, then we have $low[u] = \min\{low[u], dfn[v]\}$.

To evaluate each node in a component, we define an impact function ψ that calculates the impact of removing a node in a recursive way as in Ventresca and Aleman (2015). The impact function value $\psi(v)$ of a node $v \in \mathcal{C}$ is calculated based on two auxiliary parameters γ and η, where γ identifies the number of nodes that are descendants of v (i.e., $\phi(v)$) including v, and η indicates the sum of the node v and nodes of all new components that come from v's subtrees if removing v. It is worth noting that γ and η have the same value if v is an articulation point and is not the root node of a component, that is, $\gamma[v] = \eta[v] = \phi(v) + 1$. Let $\delta(v)$ be the set of children nodes of v in the DFS tree, and $\phi(v)$ denote the total number of nodes that are descendants of v. Then $\phi(v)$ can be recursively computed as follows:

$$\phi(v) = \sum_{w \in \delta(v)} \begin{cases} \phi(w), & \text{if } w \text{ is a root or an internal node} \\ 1, & \text{if } w \text{ is a leaf node.} \end{cases} \tag{2}$$

Once an articulation point v is removed, the component $\mathcal{C}$ is divided into two parts: ancestors and descendants. The descendants consist of multiple children subtrees that can be transformed into a series of new components. Therefore, the contribution of v's descendants to the objective function value can be calculated as follows:

$$\sum_{t_i \in T(v)} \frac{|t_i|(|t_i| - 1)}{2}, \tag{3}$$

where $|t_i|$ is the number of nodes in the children subtree $t_i \in T(v)$, and $T(v)$ is the children subtree set of v. Accordingly, the increment in the objective function can be simplified as

$$\psi[v] = f'(\mathcal{C} \setminus \{T(v) \cup \{v\}\}) + \sum_{t_i \in T(v)} \frac{|t_i|(|t_i| - 1)}{2}, \tag{4}$$

where the first part $f'(\mathcal{C} \setminus \{T(v) \cup \{v\}\})$ computes the total pairwise connectivity of the ancestors, whereas the second part presents the total pairwise connectivity of the descendants.

After traversing the component $\mathcal{C}$, a node v^* with the minimum ψ value is added to the solution S. The chosen node must be the node whose removal will maximally decrease the objective function $f(S)$. Once a node v is added into S based on the node weighting or articulation point impact strategies, that is, $S \leftarrow S \cup \{v\}$, a node u whose removal minimally deteriorates the objective function $f(S)$ is removed from S, that is, $S \leftarrow S \setminus \{u\}$. The graph changes along with the add and remove operations, accompanied by disintegration of old components and regeneration of new components.

3.4.3. Node Weighting Strategy. The node weighting strategy is an effective diversification technique for local search that has been successfully used to solve many combinational optimization problems, such as boolean satisfiability (Thornton et al. 2004) and vertex cover (Cai et al. 2011) problems. Our node weighting strategy uses an idea similar to that of the node weighting scheme used in Zhou et al. (2019). Each node of a large connected component is associated with a positive integer number as its weight. Weights are initially set to one. At each step, we select the node v from $\mathcal{C}$ with the largest weight (breaking ties randomly) to add to S. Then, the weights of the remaining nodes in $\mathcal{C}$ are incremented. Once an exchange operation is made between $v \in \mathcal{C}$ and $u \in S$, we set the weight of u to one. As the search processes, the "hard to remove" nodes of a large connected component will have larger weights, and thus have a higher chance to be selected and removed from the large connected component in subsequent search.

3.5. Common Pattern Mining

Identifying common patterns that frequently appear in a set of high-quality solutions can be naturally modeled as a frequent pattern mining task (Grahne and Zhu 2005), where common patterns refer to frequent patterns. CNP is a typical subset selection problem, its solution is usually represented as a set of removed nodes. Based on this characteristic, the problem of performing frequent pattern mining on a set of high-quality CNP solutions is reduced to mine frequent itemsets that often appear together. An itemset is composed of multiple removed nodes, and each removed node is an item. Besides itemsets, frequent patterns can also be represented as complex entities such as subsequences and substructures.

To mine useful information from high-quality solutions, considerable efforts have been made to hybridize frequent pattern mining with metaheuristic algorithms (Ribeiro et al. 2006, Plastino et al. 2014, Arnold et al. 2021, Zhou et al. 2022). A pioneer algorithm called DM-GRASP (Ribeiro et al. 2006) was proposed to solve the set packing problem, where a data mining procedure is first applied to mine useful patterns from an elite set of solutions, and then the mined pattern is used to guide the search of GRASP. MDM-GRASP (Plastino et al. 2014) improved DM-GRASP by performing data mining as soon as the elite set becomes stable (i.e., no change occurs in the elite set throughout a given number of iterations) and whenever the elite set has been changed and has become stable again, instead of performing data mining only once. Recently, Zhou et al. (2022) presented an FPBS method for the quadratic assignment problem, where frequent patterns mined from the population by FPmax* algorithm are used to guide the offspring solution construction. Although numerous frequent pattern mining algorithms are available in the literature (Luna et al. 2019), they are time consuming.

To quickly find frequent itemsets, we focus on mining common elements from only two parent solutions, randomly selecting two parent solutions S^F and S^M from the population at each generation. We observe that if all mined common elements between S^F and S^M are used to guide instance reduction, the size of the reduced instance tends to become very small. To avoid this problem and keep some randomness, we inherit each common element with a random probability. Therefore, the resulting frequent itemset ζ has no more than $\beta|S^F \cap S^M|$ elements, that is, $|\zeta| \leq \beta|S^F \cap S^M|$, where $\beta\,(0 < \beta \leq 1)$ is a proportional factor.

3.6. Reduce-Solve-Combine Mechanism

Inspired by the divide-and-conquer strategy, we propose an RSC method to generate promising offspring solutions. RSC consists of three main stages, as shown in Algorithm 4. At the reduction stage, the original instance I is reduced to I' based on a common pattern ζ (i.e., a l-itemset, where $l = |\zeta|$). All nodes of the pattern ζ and all edges associated with the nodes are deleted from the original instance I (lines 1–4). At the solution stage, from a random solution S, we apply the fast local search heuristic CHNS of Section 3.4 to find an improved solution S' for the reduced instance I' (lines 5–6). The improved solution S' can be treated as a part of the final offspring solution S^o. At the combination stage, a feasible solution of the original instance I is obtained by combining the common pattern ζ and the local optimal solution S' of I', that is, $S^o \leftarrow \zeta \cup S'$ (line 7). For some types of graphs, the reduced instance I' is usually small and can be solved by a fast exact algorithm instead of a heuristic (i.e., CHNS). Consequently, IRMS can be implemented as a matheuristic (Archetti et al. 2017, Boschetti and Maniezzo 2022).

Algorithm 4 (Pseudo Code of RSC Procedure)

```
Input: The CNP instance $I$, common pattern $\zeta$, selection probability $\theta$, and maximal idle iteration count $\hat{\xi}$
Output: An offspring solution $S^o$
    //Reduction stage
1:  for all nodes $v \in \zeta$ do
2:      $E(v) \leftarrow$ {all edges associated with $v$}
3:      $I' \leftarrow I \setminus \{v, E(v)\}$
4:  end for
    //Solution stage
5:  Randomly generate an initial solution $S'$ of $I'$
6:  $S' \leftarrow$ CHNS$(S', \theta, \hat{\xi})$
    //Combination stage
7:  $S^o \leftarrow \zeta \cup S'$
8:  return An offspring solution $S^o$
```

Figure 3 illustrates the basic idea of the RSC mechanism applied to an original instance I of 12 nodes and 16 edges with a common pattern $\zeta = \{f, g\}$. Figure 3(b) presents the reduced instance I' with 10 nodes and 9 edges by deleting all nodes of ζ and their associated edges from I. Figure 3(c) shows a high-quality local optimal solution $S' = \{c, h\}$ of I' found by CHNS. Figure 3(d) gives the feasible solution $S^o = \{f, g, c, h\}$ that is obtained by combining the common pattern $\zeta = \{f, g\}$ and the solution $S' = \{c, h\}$ of I'.

3.7. Population Updating

Following Fu and Hao (2015) and Zhou et al. (2019), we use a rank-based population updating strategy to manage the population P. Once an improved offspring solution S^o is obtained, we first tentatively insert it into P, that is, $P' \leftarrow P \cup \{S^o\}$. All $\lambda + 1$ individuals in P' are then evaluated by a combined score function $\Psi(S_i, P')$ that simultaneously considers the solution quality and solution distance. The combined score function $\Psi(S_i, P')$ can be formally defined as follows:

$$\Psi(S_i, P') = \alpha * \Phi(f(S_i)) + (1 - \alpha) * \Phi(D(S_i, P')), \tag{5}$$

where $\Phi(f(S_i))$ and $\Phi(D(S_i, P'))$ represent the rank of solution S_i with respect to its objective value f and average distance D to the population P', respectively. We rank the solutions of P' in terms of solution quality and average distance in descending order and ascending order, respectively. The parameter α is a weighting coefficient between solution quality and solution distance, which is empirically set to $\alpha = 0.6$. Afterward, the worst solution S^w with respect to the combined score function is identified, that is, $S^w \leftarrow \arg_{S_i \in P'} \min \Psi(S_i, P')$. Finally, if S^o is different from S^w, we replace S^w with S^o; otherwise, we discard S^o.

3.8. Discussion

IRMS enhances the canonical memetic algorithm framework (Neri and Cotta 2012; Zhou et al. 2023a, c) with the RSC mechanism, which benefits from the merits of both the instance reduction technique and the population-based

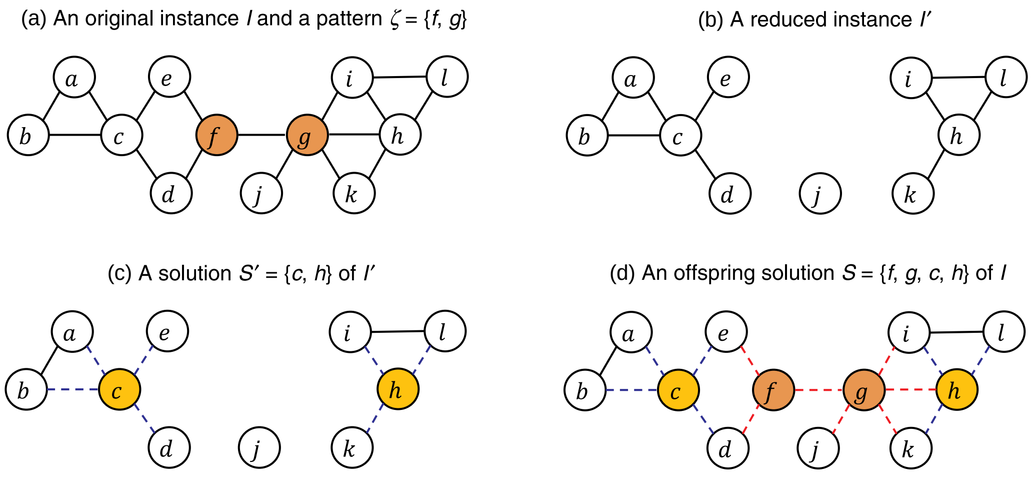
(a) An original instance I and a pattern $\zeta = \{f, g\}$
(b) A reduced instance I'
(c) A solution $S' = \{c, h\}$ of I'
(d) An offspring solution $S = \{f, g, c, h\}$ of I
a
b
c
d
e
f
g
h
i
j
k
l

Figure 3. (Color online) An Illustrative Example of the RSC Mechanism algorithm for solving large and hard CNP instances. As indicated by the review of Section 2.1, MACNP is one of the best-performing heuristic algorithms for CNP (Zhou et al. 2019). IRMS distinguishes itself from MACNP in the following four features. First, IRMS is an enhanced algorithm that integrates an instance reduction mechanism into a memetic algorithm, whereas MACNP is only a canonical memetic algorithm. Second, IRMS generates an offspring solution based on the RSC mechanism instead of the backbone-based crossover operator used in MACNP. Third, IRMS uses a CHNS to perform local optimization, which reinforces the component-based neighborhood search used in MACNP by an articulation point impact strategy. Accordingly, CBNS can be considered as a special case of CHNS, where only the node weighting strategy is applied. Finally, IRMS can use both heuristic and exact solvers to solve the reduced instances in IRMS.

Compared with existing studies on combining frequent pattern mining with metaheuristics (Ribeiro et al. 2006, Plastino et al. 2014, Arnold et al. 2021, Zhou et al. 2022), IRMS uses frequent patterns mined from high-quality solutions to guide the instance reduction instead of relying on solution construction processes. Moreover, IRMS performs instance reduction by referencing to nodes common to only two high-quality solutions instead of derived from multiple high-quality solutions as in the existing (time-consuming) frequent pattern mining algorithms (e.g., FPmax*; Grahne and Zhu 2005).

The RSC mechanism is only an algorithmic component of IRMS, whereas the reduce-optimize-expand (ROE) framework is an algorithm framework (Montiel et al. 2013). RSC distinguishes itself from ROE in three aspects. First, RSC reduces the original instance by directly removing some nodes, whereas ROE generates a reduced instance by creating fewer new nodes to represents a set of removed nodes. Second, RSC directly combines the removed nodes and the solution of the reduced instance to obtain a feasible solution of the original instance. Although ROE expands the solution of the reduced instance by inserting the discarded nodes in an additional (heuristic) way. Third, once a feasible solution of the original instance is obtained, RSC uses a local optimization procedure to further improve it to a high-quality solution.

3.9. Computational Complexity of IRMS

To analyze the computational complexity of IRMS, we consider each main module of Algorithm 1. IRMS begins its search from a high-quality initial population generated by the population initialization procedure in $O(\lambda K(|V| + |E|)\tilde{\xi})$, where λ denotes the population size, and $\tilde{\xi}$ is the total number of iterations used in CBNS.

At each generation of the main loop of Algorithm 1, IRMS sequentially executes five search procedures: parent selection, common pattern mining, RSC, CHNS, and population management. The parent selection procedure only takes time $O(1)$. A common pattern (i.e., a set of nodes) between two parent solutions can be found in $O(K)$. The RSC mechanism consists of three phases: reduction, solution and combination. Both reduction and combination phases can be executed in $O(|V|)$, and the solution phase uses CHNS to solve the reduced instance, whose complexity is $O(\xi K(|V| + |E|))$, where ξ is the total number of iterations used in CHNS. Hence, the total complexity of IRMS at each generation is $O(\xi K(|V| + |E|))$.

4. Computational Studies

4.1. Benchmark Instances and Experimental Settings

Our IRMS algorithm was implemented in C++ and compiled using GNU gcc 7.3.0 with the "-O3" option on an Intel Xeon 8269CY 16-core processor with 2.5 GHz and 32 GB RAM under the Linux system. Please refer to Zhou et al. (2023b) for the instances, codes, and results of the experiments. Our experiments are conducted on two sets of widely used benchmark instances.

- **Synthetic benchmark set** consists of 16 graphs belonging to 4 groups with different characteristics. They are generated according to four classes of commonly used complex network models: Barabási-Albert (BA), Erdős-Rényi (ER), Forest-Fire (FF), and Watts-Strogatz (WS). BA graphs are scale-free networks and proven to be the easiest to process. ER graphs are random graphs. FF graphs reproduce the behavior of how a fire spreads through a forest, with a scale-free structure like BA graphs but a denser structure. WS graphs are designed to mimic a dense small-world structure and are the most challenging to solve. The detailed characteristics of these graphs can be found in Ventresca and Aleman (2014).
- **Real-world benchmark set** is composed of 26 real-world networks from various practical applications, such as social networks, transportation networks, communication networks, biological networks, and power networks. Their details are summarized in Aringhieri et al. (2016a).

In the following experiments, we use the well-known two-tailed sign test (Demšar 2006) to check the statistical difference between the compared algorithms on each comparison indicator. At a significance level of 0.05, the

Table 2. Parameter Settings of Our IRMS Method

Parameter	Description	Considered values	Final value	Section
λ	Population size	{2,3,4,5,6,7,8,9,10}	5	3.2
$\hat{\xi}$	Maximal idle iteration count	{1,000}	1,000	3.4
θ	Selection probability	{0.2,0.3,0.4,0.5,0.6,0.7,0.8}	0.3	3.4
β	Proportional factor	{0.2,0.3,0.4,0.5,0.6,0.7,0.8,0.9,1.0}	0.9	3.5

critical value is $CV^{42}_{0.05} = N/2 + 1.96\sqrt{N}/2 \approx 27$, where N is the total number of benchmark instances, that is, $n = 42$. This implies that algorithm A statistically outperforms algorithm B if A wins in at least 27 of 42 instances.

4.2. Parameter Sensitivity Analysis

Our computational results are obtained by running IRMS with the parameter settings provided in Table 2. The parameter $\hat{\xi}$ identifies the allowable maximal idle iteration count used in CHNS. Because CHNS can be considered as an improved CBNS, we set $\hat{\xi} = 1{,}000$ as for CBNS (Zhou et al. 2019). For the values of the other three parameters, that is, population size (λ), selection probability (θ) and proportional factor (β), are determined according to common practice in heuristic algorithm design by testing a limited number of parameter configurations on representative problem instances (Cordeau et al. 2006). To identify an appropriate value for a given parameter, we allow the chosen parameter to vary, while fixing the values of other parameters.

Our parameter sensitivity analysis is conducted on a set of 10 representative instances with different sizes and variable levels of difficulty, selected from both synthetic and real-world instance sets, that is, BA5000, ER941, FF500, WS250, TreniR, open-flights, H3000a, H4000, powergrid, and OClinks. In our experiment, each parameter value varies within a range specified in the column Considered Values in Table 2, whereas the other parameters are fixed to the Final Values. The total time budget for tuning is specified to be 30 executions of IRMS for each selected instance with a limit to 100 generations.

We take the parameter sensitivity analysis of the proportional factor β as an example. Figure 4(a) and (b), shows the box plots of IRMS with different $\beta \in \{0.2, 0.3, 0.4, 0.5, 0.6, 0.7, 0.8, 0.9, 1.0\}$ values in terms of the average performance gap $\Delta\overline{f}$ and the average computation time $\overline{t}$, respectively. We calculate the performance gap as $\Delta\overline{f} = \frac{\overline{f} - \text{BKV}}{\text{BKV}}$, where BKV indicates the best-known value. From Figure 4(a), we observe that IRMS with $\beta = 0.9$ yields the best performance in terms of $\Delta\overline{f}$. We also observe that large β values ($\beta > 0.8$) have a better performance than small ones ($\beta \le 0.8$) in terms of $\overline{t}$, as shown in Figure 4(b). To make a reasonable compromise between the solution quality and computation time, we adopt $\beta = 0.9$ in IRMS.

4.3. Comparison Between IRMS and FPBS

As indicated in Zhou et al. (2022), the FPBS method tries to construct an offspring solution guided by frequent itemsets that are minded from a set of high-quality solutions by the pattern mining procedure FPmax* (Grahne and Zhu

Figure 4. (Color online) Boxplots of IRMS with Different β Values

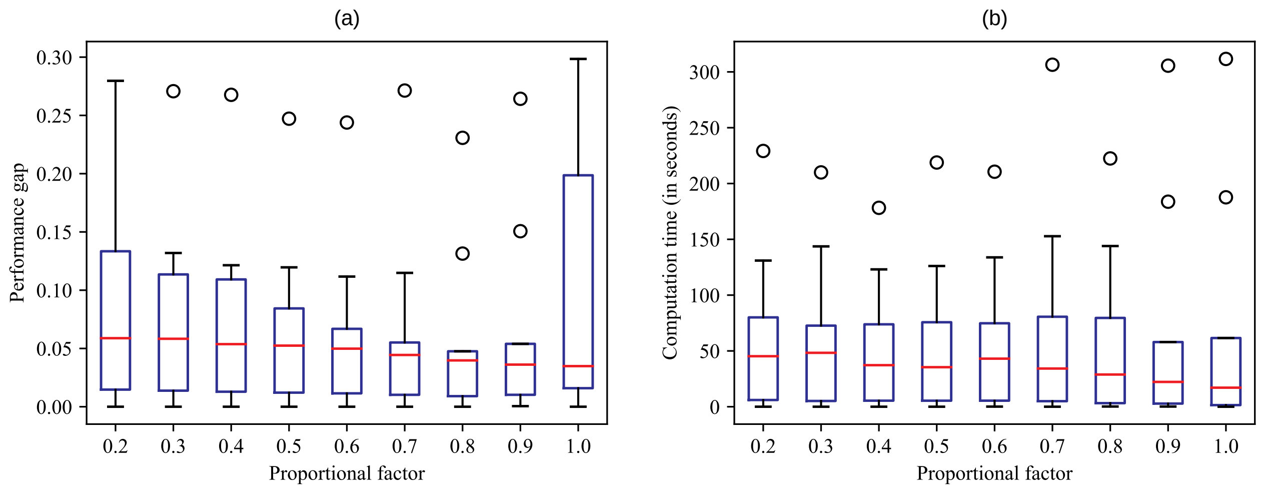

2005). Unlike FPBS, IRMS uses the mined common elements to guide the instance reduction, where the common elements are quickly identified from only two high-quality solutions. To demonstrate the superiority of IRMS, we first adapt FPBS for CNP and then experimentally compare it with IRMS. We independently solve each instance 30 times with different random seeds and set the time limit of each run at $\hat{t} = 3,600$ seconds.

Detailed comparative results between IRMS and FPBS are summarized in Table 3, where columns 1–5 present for each instance its name (Instance), number of nodes ($|V|$), K value, $K/|V|$ value, and best known value (BKV) reported in the literature. Columns 6–8 describe the detailed results of IRMS, that is, the best result ($\hat{f}$) found during 30 runs, average result ($\bar{f}$), and average computation time to attain the best result ($\bar{t}$) at each run. Similarly, columns 9–11 provide the results of FPBS. The better values of the compared results in terms of $\hat{f}$ and $\bar{f}$ are indicated in bold. In addition, we also count the number of instances in which IRMS's solution are better, equal, and worse in terms of each indicator compared with BKV and FPBS.

Table 3. Comparison Between IRMS and FPBS on Synthetic and Real-World Benchmarks Under $\hat{t} = 3,600$ Seconds

					FPBS$^\circ$			IRMS		
Instance	$\|V\|$	K	$K/\|V\|$	BKV	$\hat{f}$	$\bar{f}$	$\bar{t}$	$\hat{f}$	$\bar{f}$	$\bar{t}$
BA500	500	50	0.10	195*	**195**	**195.0**	0.0	**195**	**195.0**	0.0
BA1000	1,000	75	0.08	558*	**558**	**558.0**	28.8	**558**	**558.0**	3.1
BA2500	2,500	100	0.04	3,704*	**3,704**	**3,704.0**	3.6	**3,704**	**3,704.0**	3.9
BA5000	5,000	150	0.03	10,196*	**10,196**	**10,196.0**	20.8	**10,196**	**10,196.0**	16.8
ER235	235	50	0.21	295*	**295**	**295.0**	5.3	**295**	**295.0**	6.5
ER466	466	80	0.17	1,524.0	**1,524**	1,551.9	2,222.2	**1,524**	**1,524.0**	83.7
ER941	941	140	0.15	5,012.0	5,122.0	5,303.7	1,724.0	**5,012**	**5,020.0**	520.0
ER2344	2,344	200	0.09	902,498.0	1,006,653.0	1,035,422.4	1,451.9	**920,748**	**944,406.9**	3,146.7
FF250	250	50	0.20	194*	**194**	**194.0**	0.0	**194**	**194.0**	0.0
FF500	500	110	0.22	257*	**257**	**257.0**	1.4	**257**	**257.0**	1.4
FF1000	1,000	150	0.15	1,260*	**1,260**	**1,260.0**	95.5	**1,260**	**1,260.0**	22.2
FF2000	2,000	200	0.10	4,545*	**4,545**	4,545.5	1,810.3	**4,545**	**4,545.0**	207.3
WS250	250	70	0.28	3,083.0	3,339.0	3,542.2	1,411.6	**3,085**	**3,179.0**	2,013.2
WS500	500	125	0.25	2,072.0	2,088.0	2,123.2	2,076.1	**2,072**	**2,080.1**	297.7
WS1000	1,000	200	0.20	109,677.0	257,569.0	280,878.6	1,715.6	**138,098**	**145,969.1**	1,963.2
WS1500	1,500	265	0.18	13,098.0	13,769.0	14,256.5	1,620.1	**13,098**	**13,112.9**	2,028.7
Bovine	121	3	0.02	268.0	**268**	**268.0**	0.0	**268**	**268.0**	0.0
Circuit	252	25	0.10	2,099.0	**2,099**	**2,099.0**	13.8	**2,099**	**2,099.0**	1.3
Ecoli	328	15	0.05	806.0	**806**	**806.0**	0.0	**806**	**806.0**	0.4
USAir97	332	33	0.10	4,336.0	5,444.0	5,444.0	0.1	**4,336**	**4,648.0**	668.8
HumanDi	516	52	0.10	1,115.0	**1,115**	**1,115.0**	0.7	**1,115**	**1,115.0**	0.1
TreniR	255	26	0.10	918.0	**918**	**918.0**	0.0	**918**	**918.0**	2.5
EU_fli	1,191	119	0.10	348,268.0	350,762.0	350,887.1	1,223.9	**348,268**	**348,295.7**	998.0
openfli	1,858	186	0.10	26,783.0	29,130.0	29,778.2	1,647.0	**27,198**	**28,757.5**	1,695.8
yeast1	2,018	202	0.10	1,412.0	**1,412**	**1,412.0**	187.1	**1,412**	**1,412.0**	37.8
H1000	1,000	100	0.10	306,349.0	322,615.0	328,173.6	1,697.8	**306,349**	**308,951.9**	2,165.2
H2000	2,000	200	0.10	1,242,739.0	1,331,626.0	1,360,981.3	1,721.2	**1,236,503⋆**	**1,254,481.6**	3,028.8
H3000a	3,000	300	0.10	2,840,690.0	3,062,331.0	3,108,832.5	1,568.7	**2,804,579⋆**	**2,849,985.8**	3,088.5
H3000b	3,000	300	0.10	2,837,584.0	3,064,784.0	3,104,320.8	2,111.0	**2,801,186⋆**	**2,842,174.8**	3,164.3
H3000c	3,000	300	0.10	2,835,369.0	3,077,676.0	3,101,625.7	1,609.9	**2,801,692⋆**	**2,840,618.6**	3,066.0
H3000d	3,000	300	0.10	2,828,492.0	3,054,775.0	3,100,897.9	1,903.3	**2,816,590⋆**	**2,864,256.5**	2,940.0
H3000e	3,000	300	0.10	2,843,000.0	3,070,679.0	3,114,306.9	2,228.6	**2,836,177⋆**	**2,877,807.4**	2,715.4
H4000	4,000	400	0.10	5,038,611.0	5,541,031.0	5,591,268.4	1,489.2	**5,021,551⋆**	**5,110,687.5**	3,042.0
H5000	5,000	500	0.10	7,964,765.0	8,720,111.0	8,778,198.6	1,615.3	**8,029,837**	**8,188,900.3**	2,741.0
powergr	4,941	494	0.10	15,862.0	16,097.0	16,182.9	1,651.9	**15,866**	**15,886.6**	3,021.6
Oclinks	1,899	190	0.10	611,253.0	616,684.0	618,350.7	1,782.1	**614,467**	**614,467.6**	1,038.9
facebook	4,039	404	0.10	420,334.0	1,567,137.0	1,602,706.4	2,183.0	**719,722**	**741,314.4**	2,852.1
grqc	5,242	524	0.10	13,591.0	13,673.0	13,708.7	2,463.1	**13,594**	**13,613.0**	3,201.9
hepth	9,877	988	0.10	106,276.0	122,109.0	132,995.7	2,181.8	**115,133**	**119,766.8**	3,159.4
hepph	12,008	1,201	0.10	6,155,877.0	11,300,876.0	11,957,556.6	1,432.2	**9,401,029**	**9,781,789.8**	3,077.4
astroph	18,772	1,877	0.10	53,963,375.0	61,896,814.0	62,977,189.9	1,880.7	**57,592,461**	**58,649,781.0**	3,271.4
condmat	23,133	2,313	0.10	2,298,596.0	9,950,262.0	10,890,742.9	2,254.0	**9,670,268**	**10,789,125.6**	2,286.2
No. of wins|ties|loses				7|22|13	26|16|0	28|14|0	–	–	–	–

Notes. The best values are highlighted in bold. * presents the optimal solution; ⋆ indicates the improved best upper bounds, and ∘ indicates an application of the FPBS (Zhou et al. 2022) method for CNP.

It is worth noting that (1) the tested instances have been studied for a long time since year 2009 (Arulselvan et al. 2009); (2) the current best known results have been improved progressively by a number of algorithms (Arulselvan et al. 2009; Ventresca 2012; Pullan 2015; Addis et al. 2016; Aringhieri et al. 2016a, b; Purevsuren et al. 2017; Veremyev et al. 2019; Zhou et al. 2019, 2021b; de San Lázaro et al. 2021; Wang and Di 2022), and (3) no single algorithm can attain all best known results. Thus, it is challenging to further improve the current best-known results, even by a small order.

From Table 3, we observe that IRMS demonstrates an excellent performance by finding new upper bounds for seven instances (marked by $\star$) and matching the best-known upper bounds on 22 instances. Compared with FPBS, IRMS finds better results in terms of $\hat{f}$ on 26 of 42 instances and matches best-known values on the remaining 16 instances except for the instance astroph. For the $\overline{f}$ performance indicator, IRMS also shows a better performance by attaining 28 better results and 14 equal results. At a significance level of 0.05, IRMS is significantly better than FPBS both in terms of $\hat{f}$ (i.e., $34.0 > CV^{42}_{0.05}$) and $\overline{f}$ (i.e., $35.0 > CV^{42}_{0.05}$).

4.4. Comparison with State-of-the-Art Algorithms

To further evaluate IRMS, we conduct a detailed comparison with four state-of-the-art algorithms, that is, CAN1 (Pullan 2015), MACNP (Zhou et al. 2019), VPMS (Zhou et al. 2021b), and CEMCNP (Wang and Di 2022). To the best of our knowledge, these four methods are the best-performing algorithms for CNP in the literature, and they attain the best-known values available except for the facebook and condmat instances.[1] Because the source code and executable program of CEMCNP are not available to us, we reimplemented the method based on its pseudo code (Wang and Di 2022). Detailed comparisons between the reported results and computational results of CEMCNP are summarized in the online appendix (Zhou et al. 2023b). To guarantee a fair comparison, we run IRMS and these four algorithms (with their source codes) on the same computational platform and under the same time limit $\hat{t}$. Table 4 summarizes the detailed results between IRMS and these state-of-the-art algorithms on synthetic and real-world benchmark instances under the time limit $\hat{t} = 3{,}600$ seconds.

From Table 4, we observe that IRMS competes very favorably with these state-of-the-art algorithms by attaining seven new upper bounds and matching 22 best-known upper bounds. At a significance level of 0.05, IRMS significantly outperforms CAN1 both in terms of $\hat{f}$ (i.e., $33.0 > CV^{42}_{0.05} = 27.0$) and $\overline{f}$ (i.e., $36.0 > CV^{42}_{0.05}$). For the comparison between MACNP and IRMS, we can obtain similar observations. That is, IRMS is significantly better than MACNP in terms of $\hat{f}$ (i.e., $27.5 > CV^{42}_{0.05}$), and it also outperforms MACNP in terms of $\overline{f}$ (i.e., $30.0 > CV^{42}_{0.05}$). Compared with VPMS, IRMS wins in 26.0 instances in terms of $\hat{f}$, which is just slightly smaller than the critical value $CV^{42}_{0.05} = 27.0$. For the $\overline{f}$ indicator, IRMS significantly outperforms VPMS, that is, $29.0 > CV^{42}_{0.05}$. For the comparison between IRMS and CEMCNP, we find that IRMS significantly outperforms CEMCNP both in terms of $\hat{f}$ (i.e., $32.5 > CV^{42}_{0.05}$) and $\overline{f}$ (i.e., $35.5 > CV^{42}_{0.05}$). These observations show that IRMS is highly effective compared with the state-of-the-art algorithms.

To further demonstrate the performance of IRMS, we report detailed results of IRMS under the longer time limit $\hat{t} = 7{,}200$ seconds in Table 1 of the online appendix (Zhou et al. 2023b). We observe that IRMS improves its results with this extended time limit by finding two new upper bounds for the instances H5000 and grqc.

Finally, IRMS has trouble to attain the best known results for facebook and condmat. Conversely, we observe that these instances are challenging for almost all algorithms, except the ILS-N$_1$-FC algorithm of Aringhieri et al. (2016b), which reported the current best-known results for these two instances (under the time limits of 3,000 and 16,000 seconds, respectively) but does not perform so well on a number of other instances, as shown in table 5 of Aringhieri et al. (2016a).

5. Application to the Node-Weighted Critical Node Problem

To show that our IRMS method may be applied to solve other optimization problems, we consider the node-weighted critical node problem (NWCNP) (Chen et al. 2020, Zhou et al. 2021a), which consists of minimizing the pairwise connectivity of a given node-weighted graph by removing a subset of nodes subject to a budgetary constraint. We start with an introduction of NWCNP, followed by reporting detailed comparative results between IRMS and existing methods.

5.1. Node-Weighted Critical Node Problem

NWCNP is a node-weighted version of CNP, which aims to minimize the objective function (1) and CNP and simultaneously satisfies the following budgetary constraint (6):

$$\text{Subset to} \sum_{i=1}^{|S|} w(v_{S(i)}) \leq K, \tag{6}$$

where the terms $w(v_{S(i)}) > 0$ are positive weights associated with each node, and $K > 0$ is a predefined budget limit.

Table 4. Comparison Between IRMS and State-of-the-Art Algorithms on Synthetic and Real-World Benchmarks Under $\hat{t} = 3,600$ Seconds

			CAN1°		MACNP°		VPMS°		CEMCNP°		IRMS	
Instance	K	BKV	$\hat{f}$	$\bar{f}$	$\hat{f}$	$\bar{f}$	$\hat{f}$	$\bar{f}$	$\hat{f}$	$\bar{f}$	$\hat{f}$	$\bar{f}$
BA500	50	195*	**195**	**195.0**	**195**	**195.0**	**195**	**195.0**	**195**	**195.0**	**195**	**195.0**
BA1000	75	558*	**558**	558.1	**558**	**558.0**	**558**	**558.0**	**558**	**558.0**	**558**	**558.0**
BA2500	100	3,704*	**3,704**	**3,704.0**	**3,704**	**3,704.0**	**3,704**	**3,704.0**	**3,704**	**3,704.0**	**3,704**	**3,704.0**
BA5000	150	10,196*	**10,196**	**10,196.0**	**10,196**	**10,196.0**	**10,196**	**10,196.0**	**10,196**	**10,196.0**	**10,196**	**10,196.0**
ER235	50	295	**295**	**295.0**	**295**	**295.0**	**295**	**295.0**	297	302.8	**295**	**295.0**
ER466	80	1,524	**1,524**	1,524.4	**1,524**	**1,524.0**	**1,524**	**1,524.0**	1,569	1,630.6	**1,524**	**1,524.0**
ER941	140	5,012	5,102	5,221.7	**5,012**	**5,014.5**	**5,012**	5,030.6	5,363	5,635.3	**5,012**	5,020.0
ER2344	200	902,498	993,035	1,010,337.9	**905,472**	**922,882.6**	909,510	938,362.3	1,012,527	1,060,618.6	920,748	944,406.9
FF250	50	194*	**194**	**194.0**	**194**	**194.0**	**194**	**194.0**	**194**	**194.0**	**194**	**194.0**
FF500	110	257*	262	265.2	**257**	**257.0**	**257**	**257.0**	**257**	258.6	**257**	**257.0**
FF1000	150	1,260*	1,262	1,266.1	**1,260**	1,260.1	**1,260**	**1,260.0**	**1,260**	**1,260.0**	**1,260**	**1,260.0**
FF2000	200	4,545*	4,548	4,551.9	**4,545**	4,545.6	**4,545**	**4,545.0**	4,546	4,552.5	**4,545**	**4,545.0**
WS250	70	3,083	3,491	3,820.7	**3,083**	3,114.5	**3,083**	**3,090.6**	4,203	5,447.9	3,085	3,179.0
WS500	125	2,072	2,086	2,102.5	**2,072**	2,084.1	2,081	2,084.9	2,085	2,193.0	**2,072**	**2,080.1**
WS1000	200	109,677	138,212	159,031.0	115,075	**136,374.1**	**114,066**	140,033.7	154,899	169,877.2	138,098	145,969.1
WS1500	265	13,098	13,784	13,997.7	13,103	13,203.5	**13,098**	13,216.4	13,664	27,810.6	**13,098**	**13,112.9**
Bovine	3	268	**268**	**268.0**	**268**	**268.0**	**268**	**268.0**	**268**	**268.0**	**268**	**268.0**
Circuit	25	2,099	**2,099**	**2,099.0**	**2,099**	**2,099.0**	**2,099**	**2,099.0**	2,101	2,188.7	**2,099**	**2,099.0**
Ecoli	15	806	**806**	**806.0**	**806**	**806.0**	**806**	**806.0**	**806**	808.8	**806**	**806.0**
USAir97	33	4,336	**4,336**	**4,336.0**	**4,336**	4,372.1	**4,336**	5,175.4	**4,336**	5,149.5	**4,336**	4,648.0
humanDi	52	1,115	**1,115**	**1,115.0**	**1,115**	**1,115.0**	**1,115**	**1,115.0**	**1,115**	**1,115.0**	**1,115**	**1,115.0**
TreniR	26	918	**918**	**918.0**	**918**	**918.0**	**918**	**918.0**	**918**	**918.0**	**918**	**918.0**
EU_fli	119	348,268	**348,268**	348,334.3	**348,268**	353,026.5	**348,268**	350,180.1	350,762	357,502.7	**348,268**	**348,295.7**
openfli	186	26,783	29,534	30,149.7	28,560	28,808.2	**26,874**	**28,283.6**	29,481	31,377.7	27,198	28,757.5
yeast1	202	1,412	1,416	1,418.6	**1,412**	**1,412.0**	**1,412**	**1,412.0**	**1,412**	1,414.3	**1,412**	**1,412.0**
H1000	100	306,349	315,911	318,845.9	306,960	311,398.7	307,117	310,827.9	330,493	337,217.0	**306,349**	**308,951.9**
H2000	200	1,242,739	1,274,815	1,294,724.6	1,251,076	1,272,246.2	1,242,907	1,258,529.7	1,324,988	1,344,914.2	**1,236,503⋆**	**1,254,481.6**
H3000a	300	2,840,690	2,914,000	2,927,166.6	2,885,246	2,922,682.4	2,849,192	2,877,853.3	2,962,661	3,042,695.4	**2,804,579⋆**	**2,849,985.8**
H3000b	300	2,837,584	2,902,347	2,926,677.7	2,870,707	2,927,682.0	2,839,130	2,863,625.1	2,968,601	3,035,272.7	**2,801,186⋆**	**2,842,174.8**
H3000c	300	2,835,369	2,899,932	2,926,225.4	2,863,929	2,909,535.2	2,837,599	2,861,449.2	2,956,916	3,008,793.3	**2,801,692⋆**	**2,840,618.6**
H3000d	300	2,828,492	2,899,196	2,930,428.5	2,865,406	2,924,250.5	2,833,030	2,870,559.0	2,967,747	3,030,236.3	**2,816,590⋆**	**2,864,256.5**
H3000e	300	2,843,000	2,919,830	2,937,228.7	2,875,727	2,934,267.0	2,845,660	**2,876,424.3**	3,012,046	3,043,889.5	**2,836,177⋆**	2,877,807.4
H4000	400	5,038,611	5,196,850	5,241,007.7	5,211,868	5,322,566.9	5,098,049	5,186,904.9	5,261,850	5,383,301.3	**5,021,551⋆**	**5,110,687.5**
H5000	500	7,964,765	8,181,618	8,221,915.3	8,369,202	8,506,623.6	8,078,843	8,217,193.6	8,206,499	8,348,589.5	**8,029,837**	**8,188,900.3**
powergr	494	15,862	16,141	16,276.4	15,882	15,917.5	15,957	16,014.3	15,965	16,084.9	**15,866**	**15,886.6**
Oclinks	190	611,253	**611,352**	614,711.5	614,467	614,728.9	612,314	615,030.6	622,237	626,701.5	614,467	**614,467.6**
facebook	404	420,334	**675,630**	754,777.4	711,505	785,554.5	713,625	794,649.1	794,938	857,245.1	719,722	**741,314.4**
grqc	524	13,591	15,544	15,874.9	13,599	13,632.4	13,628	13,666.4	13,666	13,701.7	**13,594**	**13,613.0**
hepth	988	106,276	136,635	221,421.8	124,269	132,192.5	115,168	120,040.4	**109,504**	**111,495.6**	115,133	119,766.8
hepph	1,201	6,155,877	10,059,965	10,724,290.3	11,114,770	11,972,968.7	9,664,750	10,580,257.6	**8,464,199**	10,530,358.9	9,401,029	**9,781,789.8**
astroph	1,877	53,963,375	60,078,332	61,679,547.3	61,667,966	62,931,865.7	59,811,734	61,171,775.9	59,476,077	60,449,655.3	**57,592,461**	**58,649,781.0**
condmat	2,313	2,298,596	14,140,443	15,233,424.7	10,101,966	10,829,853.5	11,141,111	12,186,050.0	**3,756,761**	**4,632,078.6**	9,670,268	10,789,125.6
No. of wins|ties|loses		–	26|14|2	31|10|1	17|21|4	23|14|5	16|20|6	21|16|5	26|13|3	31|9|2	–	–

Notes. The best values are highlighted in bold. * presents the optimal solution, ⋆ indicates the improved best upper bounds, and ∘ indicates the results of CNA1, MACNP, and VPMS obtained by executing their source codes, whereas the results of CEMCNP are obtained by executing our reimplemented CEMCNP algorithm, which are slightly different from their reported results.

CNP can be considered as a special case of NWCNP where the weight of each node is set to one, that is, $w(v_i) = 1,\ \forall v_i \in V$. As pointed out by Zhou et al. (2021a), an optimal solution of CNP is not necessarily optimal for NWCNP, and NWCNP is at least as challenging computationally as CNP (Arulselvan et al. 2009). Recently, some efforts have been devoted to solve it. For example, Chen et al. (2020) studied CNP in undirected weighted networks and proposed a mixed-integer quadratic programming model and a greedy algorithm. Zhou et al. (2021a) introduced an iterative local search algorithm (ILS-NWCNP for short) by iterating through a late acceptance-based local search and a destructive-constructive perturbation, which achieved the state-of-the-art results for NWCNP.

5.2. Computational Results on NWCNP

As benchmark instances for NWCNP are not available, we generated new weighted instances starting from the widely used synthetic and real-world CNP benchmarks. The only information required to be added is the weighting information for each node in the sparse graph. Following Zhou et al. (2021a), we adopt a random weighting scheme to assign a weight to each node given by $w(v_i) \in [0.2, 3],\ \forall v_i \in V$. Please refer to Zhou et al. (2023b) for both our implemented programs and generated benchmark instances.

To adapt IRMS to solve NWCNP, some modifications to main algorithmic modules (e.g., solution initialization and CHNS) of IRMS are necessary. According to the budgetary constraint (6), a feasible solution of NWCNP must satisfy the constraint dictating that the total weight of all removed nodes should be no more than K. Therefore, an initial solution is constructed by iteratively removing nodes from the graph until the total weight of all removed nodes is larger than K. A feasible solution of NWCNP is not necessary to have K nodes. In addition, at each iteration, CHNS selects a removed node according to both impact function value ψ and node weight w instead of value ψ only.

We use IRMS-NWCNP to denote the resulting IRMS algorithm for NWCNP. The source code of ILS-NWCNP is available to us, which is responsible for achieving most of state-of-the-art results for NWCNP in the literature. Although for CEM-NWCNP, it is a new adaption of CEMCNP (Wang and Di 2022) for NWCNP. Correspondingly, the resulting algorithm for NWCNP is denoted as CEM-NWCNP. Therefore, we focus on experimentally comparing IRMS-NWCNP with both ILS-NWCNP and CEM-NWCNP and report the results in Table 5.

From Table 5, we observe that IRMS-NWCNP outperforms ILS-NWCNP in terms of both $\hat{f}$ and $\overline{f}$, finding better $\hat{f}$ values for 37 instances, and equal $\hat{f}$ values for 2 of the 5 remaining instances. In terms of $\overline{f}$, IRMS-NWCNP achieves better results than ILS-NWCNP except for three instances (i.e., WS1000, WS1500, and facebook). At a significance level of 0.05, IRMS-NWCNP significantly outperforms ILS-NWCNP in terms of both $\hat{f}$ (i.e., $38 > CV^{42}_{0.05}$) and $\overline{f}$ (i.e., $39 > CV^{42}_{0.05}$). Compared with CEM-NWCNP, IRMS-NWCNP also shows better performance. At a significance level of 0.05, IRMS-NWCNP is significantly better than CEM-NWCNP in terms of $\hat{f}$, that is, $34.5 > CV^{42}_{0.05}$. Although for the performance indicator $\overline{f}$, IRMS-NWCNP also significantly outperforms CEM-NWCNP (i.e., $37.5 > CV^{42}_{0.05}$).

6. Experimental Analysis

In this section, we perform additional testing to gain a deeper understanding of IRMS by conducting three groups of experiments: (1) to study the run-time distributions of IRMS and state-of-the-art algorithms, (2) to investigate the benefit of the component-based hybrid neighborhood search procedure, and (3) to confirm the effectiveness of the RSC mechanism.

6.1. Run-Time Distributions of IRMS and State-of-the-Art Algorithms

To further compare IRMS with the three state-of-the-art algorithms, we use time-to-target (TTT) plots (Aiex et al. 2007) to show the algorithmic run-time distributions on representative instances. We execute each algorithm 100 times for each instance and record the computation time to obtain a solution at least as good as a given target value at each run. The 100 computation times are sorted in ascending order, and a probability $p_i = \frac{i-0.5}{100}$ is associated with the ith sorted computation time t_i. A TTT plot is then obtained by plotting these 100 points $(t_i, p_i), i = 1, 2, \ldots, 100$. Figure 5 presents the TTT plots of IRMS and the three state-of-the-art algorithms on four representative instances, that is, BA1000 (10,196), FF1000 (1,271), humanDi (1,115), and yeast1 (1,421). The target value of each instance is indicated in the parentheses after each instance name.

From Figure 5, we observe that IRMS is likely to find a target solution faster than the compared algorithms. For example, for the synthetic instance BA1000, the probability of reaching the target value 10,196 in at most 130 seconds is approximately 60% for both CAN1 and VPMS and 100% for both MACNP and IRMS. For the real-world instance humanDi, the probability of finding the target value 1,115 in at most five seconds is approximately 40% for CAN1, 50% for VPMS, and 75% for MACNP, whereas it is at least 95% for IRMS. These observations further confirm that IRMS outperforms the state-of-the-art algorithms.

Table 5. Comparison Between IRMS-NWCNP and Reference Algorithms on Weighted Synthetic and Real-World Benchmarks Under $\hat{t} = 3,600$ Seconds

		ILS-NWCNP$^\circ$			CEM-NWCNP			IRMS-NWCNP		
Instance	K	$\hat{f}$	$\bar{f}$	$\bar{t}$	$\hat{f}$	$\bar{f}$	$\bar{t}$	$\hat{f}$	$\bar{f}$	$\bar{t}$
BA500	50	283	286.7	65.0	278	280.7	1.1	**269**	**271.4**	1,946.1
BA1000	75	820	835.8	703.4	819	829.3	3.2	**815**	**823.4**	2,098.5
BA2500	100	4,910	4,973.2	1,153.1	**4,784**	4,909.7	55.8	4,825	**4,884.4**	2,544.0
BA5000	150	13,722	13,907.4	162.6	**13,346**	**13,640.3**	535.3	13,672	13,797.1	2,600.0
ER235	50	724	1,495.7	680.4	922	1,591.0	0.2	**616**	**638.0**	2,081.8
ER466	80	19,104	23,745.6	92.8	19,870	27,351.1	0.6	**4,274**	**5,117.9**	1,989.0
ER941	140	63,079	78,285.9	1,407.5	55,194	78,522.3	35.7	**38,654**	**43,229.0**	3,073.9
ER2344	200	1,397,614	1,491,688.6	2,885.2	1,495,253	1,629,017.5	69.5	**1,334,743**	**1,355,718.0**	2,845.2
FF250	50	479	514.8	196.3	522	547.0	0.1	**466**	**475.2**	1,661.5
FF500	110	532	556.4	356.9	561	580.4	1.5	**514**	**525.5**	2,992.4
FF1000	150	2,469	2,509.1	1,918.0	**2,345**	2,494.5	11.5	2,374	**2,402.1**	2,912.4
FF2000	200	8,715	8,822.4	824.0	**7,837**	**8,212.2**	180.2	8,435	8,535.9	2,731.7
WS250	70	8,801	10,270.9	414.2	9,724	14,414.2	205.8	**8,304**	**8,468.5**	1,408.9
WS500	125	5,924	6,553.2	785.4	13,810	25,821.4	4.2	**4,679**	**5,049.9**	3,081.1
WS1000	200	**222,092**	**228,611.7**	2,048.3	277,755	311,422.1	628.7	247,187	260,977.6	2,721.2
WS1500	265	**78,142**	**95,715.1**	2,577.0	236,725	344,796.0	58.9	134,518	158,567.2	2,409.3
Bovine	3	**954**	954.6	237.5	**954**	**954.0**	0.0	**954**	**954.0**	0.1
Circuit	25	3,498	4,254.6	395.8	4,718	7,253.7	0.1	**3,160**	**3,204.0**	1,826.1
Ecoli	15	**1,348**	1,360.0	759.4	1,368	1,591.4	0.3	**1,348**	**1,348.0**	0.5
USAir97	33	9,484	9,545.0	865.5	9,441	9,955.0	0.7	**9,313**	**9,345.1**	978.3
humanDi	52	1,843	1,867.2	575.7	1,727	1,826.1	2.0	**1,693**	**1,700.7**	1,824.5
TreniR	26	647	648.8	962.9	627	695.3	0.6	**597**	**634.7**	2,537.0
EU_flights	119	395,636	399,652.6	955.0	400,991	407,205.3	75.3	**386,809**	**388,392.8**	2,144.6
openflights	186	91,072	95,801.6	2,093.8	95,097	103,457.7	183.6	**87,420**	**87,939.6**	2,474.7
yeast1	202	3,569	3,700.2	1,344.7	3,320	3,495.9	206.2	**3,317**	**3,373.0**	2,917.6
H1000	100	345,971	353,678.8	1,005.0	381,567	398,257.1	168.7	**317,208**	**325,771.1**	2,908.5
H2000	300	1,412,216	1,444,356.3	490.4	1,574,504	1,608,151.6	743.4	**1,331,567**	**1,356,273.3**	2,889.0
H3000a	300	3,146,558	3,234,620.3	1,654.6	3,581,933	3,690,692.4	899.9	**3,098,206**	**3,133,268.5**	2,755.0
H3000b	300	3,169,598	3,224,242.6	1,214.0	3,614,080	3,679,776.8	1,056.7	**3,047,488**	**3,077,125.0**	2,991.0
H3000c	300	3,180,822	3,224,308.1	1,892.6	3,523,237	3,650,634.8	759.3	**3,074,841**	**3,118,908.1**	2,553.1
H3000d	300	3,159,049	3,205,091.0	1,519.1	3,499,408	3,635,271.7	970.8	**3,089,828**	**3,124,039.0**	2,875.4
H3000e	300	3,156,667	3,221,055.5	1,160.7	3,630,227	3,660,257.7	1,282.0	**3,097,630**	**3,145,617.3**	2,877.8
H4000	400	5,650,385	5,712,357.8	2,014.2	6,435,143	6,539,854.0	1,428.0	**5,563,646**	**5,629,050.2**	2,868.9
H5000	500	8,915,291	8,999,620.4	2,593.4	10,190,504	10,268,278.5	1,724.9	**8,799,566**	**8,950,070.3**	2,973.4
powergrid	494	36,639	41,493.8	2,019.5	**28,702**	**30,541.8**	2,479.8	36,395	37,144.5	2,793.2
Oclinks	190	798,262	807,393.5	1,991.5	812,214	826,705.5	604.8	**775,689**	**782,060.6**	2,851.2
facebook	404	**1,444,026**	**1,469,417.4**	3,095.0	1,444,559	2,011,511.2	2,224.1	1,570,192	1,585,472.6	2,862.8
grqc	524	47,604	52,548.5	1,720.8	**41,914**	**46,216.3**	2,381.1	44,664	47,360.7	2,747.7
hepth	988	8,016,122	8,225,523.5	3,436.0	8,924,436	9,908,367.9	3,524.0	**6,934,032**	**7,070,319.2**	2,714.5
hepph	1,201	25,775,334	26,101,767.5	3,399.9	28,084,670	30,582,642.5	3,361.6	**23,594,695**	**24,177,629.2**	2,851.7
astroph	1,877	82,976,199	84,203,164.2	3,568.2	96,874,011	100,752,411.9	3,532.4	**77,314,231**	**78,730,627.0**	2,991.2
condmat	2,313	72,014,730	75,003,163.3	3,555.2	93,241,452	97,411,338.5	3,580.1	**60,805,637**	**66,817,701.5**	3,365.8
No. of wins|ties|loses		37|2|3	39|0|3	–	34|1|7	37|1|4	–	–	–	–

Notes. The best values are highlighted in bold. ∘ presents the results of ILS-NWCNP obtained by executing its source code in our computational platform.

6.2. Benefit of the Component-Based Hybrid Neighborhood Search

As previously noted, IRMS uses CHNS to perform local optimization, using the articulation point impact strategy to improve on the CBNS algorithm (Zhou et al. 2019). To show the benefit of CHNS, we experimentally compare IRMS with a variant named IRMS′ that is obtained from IRMS by replacing CHNS with CBNS. That is, IRMS′ selects a node based on the node weighting strategy rather than the articulation point impact strategy during the search. Detailed comparative results between IRMS′ and IRMS on both the synthetic and real-world benchmarks are summarized in Table 6.

Table 6 shows that IRMS dominates IRMS′ by achieving better results on 19 instances and equal results on the 22 remaining instances in terms of $\hat{f}$. IRMS statistically beats IRMS′ on 30.0 instances (i.e., $30.0 > CV^{42}_{0.05}$) at a significance level of 0.05. For the $\bar{f}$ indicator, IRMS finds better results on 24 instances and equal results on the 16 remaining instances. At a significance level of 0.05, IRMS significantly outperforms IRMS′ (i.e., $32.0 > CV^{42}_{0.05}$). These results confirm the benefit of CHNS over CBNS.

Figure 5. (Color online) TTT Plots of IRMS and State-of-the-art Algorithms

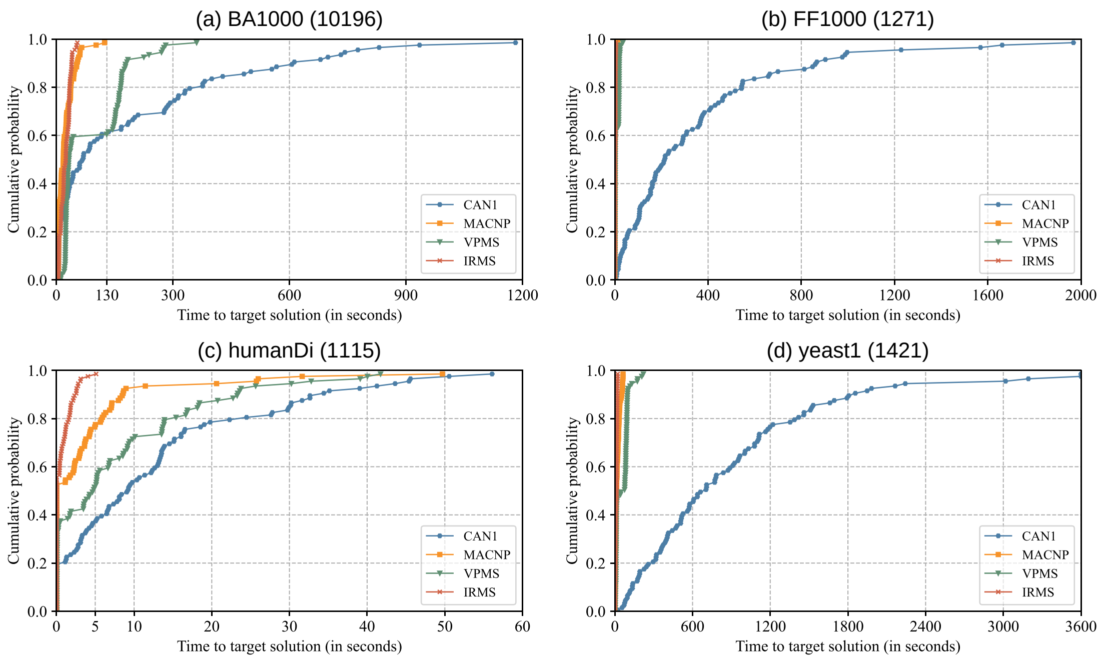

6.3. Effectiveness of the RSC Mechanism

To evaluate the effectiveness of the RSC mechanism used by IRMS, we compare IRMS with an alternative version called IRMS″ obtained from IRMS by disabling the RSC mechanism and directly constructing an offspring solution based on the frequent pattern and the offspring construction method used in frequent pattern based search (Zhou et al. 2022). Table 7 describes the comparative results between IRMS and IRMS″ on both the synthetic and real-world instances under the time limit $\hat{t} = 3,600$ seconds.

As seen from Table 7, IRMS demonstrates a better performance than IRMS″ by obtaining better results on 21 instances and equal results on the 21 remaining instances in terms of $\hat{f}$. Similar observations apply to the $\overline{f}$ indicator, where IRMS attains the same or better results on all 42 instances except for the instance Oclinks. At a significance

Table 6. Comparison Between IRMS and IRMS′ on Synthetic and Real-World Benchmarks Under $\hat{t} = 3,600$ Seconds

			IRMS′			IRMS		
Instance	K	BKV	$\hat{f}$	$\overline{f}$	$\overline{t}$	$\hat{f}$	$\overline{f}$	$\overline{t}$
BA500	50	195*	**195**	**195.0**	0.0	**195**	**195.0**	0.0
BA1000	75	558*	**558**	**558.0**	1.3	**558**	**558.0**	3.1
BA2500	100	3,704*	**3,704**	**3,704.0**	5.3	**3,704**	**3,704.0**	3.9
BA5000	150	10,196*	**10,196**	**10,196.0**	15.8	**10,196**	**10,196.0**	16.8
ER235	50	295	**295**	**295.0**	2.8	**295**	**295.0**	6.5
ER466	80	1,524	**1,524**	**1,524.0**	651.6	**1,524**	**1,524.0**	83.7
ER941	140	5,012	**5,012**	5,048.1	1,724.0	**5,012**	**5,020.0**	520.0
ER2344	200	902,498	929,333	951,425.0	3,010.4	**920,748**	**944,406.9**	3,146.7
FF250	50	194*	**194**	**194.0**	0.1	**194**	**194.0**	0.0
FF500	110	257*	**257**	**257.0**	0.8	**257**	**257.0**	1.4
FF1000	150	1,260*	**1,260**	**1,260.0**	27.0	**1,260**	**1,260.0**	22.2
FF2000	200	4,545*	**4,545**	**4,545.0**	115.4	**4,545**	**4,545.0**	207.3
WS250	70	3,083	3,324	3,600.2	2,067.5	**3,085**	**3,179.0**	2,013.2
WS500	125	2,072	**2,072**	**2,079.0**	436.4	**2,072**	2,080.1	297.7
WS1000	200	109,677	244,708	274,428.2	1,567.4	**138,098**	**145,969.1**	1,963.2
WS1500	265	13,098	13,100	13,121.2	1,670.6	**13,098**	**13,112.9**	2,028.7
Bovine	3	268	**268**	**268.0**	0.0	**268**	**268.0**	0.0

Table 6. (Continued)

			IRMS′			IRMS		
Instance	K	BKV	$\hat{f}$	$\bar{f}$	$\bar{t}$	$\hat{f}$	$\bar{f}$	$\bar{t}$
Circuit	25	2,099	**2,099**	**2,099.0**	0.8	**2,099**	**2,099.0**	1.3
Ecoli	15	806	**806**	**806.0**	0.0	**806**	**806.0**	0.4
USAir97	33	4,336	**4,336**	4,736.9	1,365.0	**4,336**	**4,648.0**	668.8
HumanDi	52	1,115	**1,115**	**1,115.0**	4.4	**1,115**	**1,115.0**	0.1
TreniR	26	918	**918**	**918.0**	1.8	**918**	**918.0**	2.5
EU_fli	119	348,268	**348,268**	349,321.2	1,683.3	**348,268**	**348,295.7**	998.0
openfli	186	26,783	28,718	28,880.0	1,946.7	**27,198**	**28,757.5**	1,695.8
yeast1	202	1,412	**1,412**	**1,412.0**	51.9	**1,412**	**1,412.0**	37.8
H1000	100	306,349	308,299	310,940.3	2,576.1	**306,349**	**308,951.9**	2,165.2
H2000	200	1,242,739	1,271,562	1,310,345.4	2,422.2	**1,236,503**	**1,254,481.6**	3,028.8
H3000a	300	2,840,690	2,914,963	2,992,166.4	2,528.1	**2,804,579**	**2,849,985.8**	3,088.5
H3000b	300	2,837,584	2,929,494	3,011,990.2	2,692.4	**2,801,186**	**2,842,174.8**	3,164.3
H3000c	300	2,835,369	2,925,015	2,983,251.7	2,343.5	**2,801,692**	**2,840,618.6**	3,066.0
H3000d	300	2,828,492	2,938,989	3,007,547.3	2,451.9	**2,816,590**	**2,864,256.5**	2,940.0
H3000e	300	2,843,000	2,960,196	3,014,327.4	2,783.2	**2,836,177**	**2,877,807.4**	2,715.4
H4000	400	5,038,611	5,313,533	5,421,596.1	2,641.3	**5,021,551**	**5,110,687.5**	3,042.0
H5000	500	7,964,765	8,297,260	8,575,610.7	2,392.2	**8,029,837**	**8,188,900.3**	2,741.0
powergr	494	15,862	**15,866**	15,891.3	3,171.9	**15,866**	**15,886.6**	3,021.6
Oclinks	190	611,253	**614,467**	614,651.4	1,676.8	**614,467**	**614,467.6**	1,038.9
facebook	404	420,334	919,158	1,258,604.9	2,991.4	**719,722**	**741,314.4**	2,852.1
grqc	524	13,591	13,601	13,626.6	3,147.3	**13,594**	**13,613.0**	3,201.9
hepth	988	106,276	116,527	**119,693.3**	3,228.1	**115,133**	119,766.8	3,159.4
hepph	1,201	6,155,877	11,353,914	11,951,940.6	2,447.0	**9,401,029**	**9,781,789.8**	3,077.4
astroph	1,877	53,963,375	62,237,249	63,050,133.4	2,242.8	**57,592,461**	**58,649,781.0**	3,271.4
condmat	2,313	2,298,596	**9,642,594**	10,902,735.5	2,233.3	9,670,268	**10,789,125.6**	2,286.2
No. of wins|ties|loses	–	–	19|22|1	24|16|2	–	–	–	–

Notes. The best values are highlighted in bold. * presents the optimal solution.

level of 0.05, IRMS significantly outperforms IRMS″ in terms of both the $\hat{f}$ (i.e., $31.5 > CV^{42}_{0.05}$) and $\bar{f}$ (i.e., $33.0 > CV^{42}_{0.05}$) indicators, confirming the effectiveness of RSC.

7. Conclusion

Finding an optimal set of nodes, called critical nodes, whose removal will maximally decrease the pairwise connectivity of the remaining graph, is a fundamental critical node detection problem. To solve this problem, we propose an instance reduction-based memetic search (IRMS) method that integrates a reduce-solve-combine instance reduction mechanism with the well-known population-based memetic algorithm framework. Extensive experimental results on 42 synthetic and real-world benchmark instances show that IRMS is highly effective compared with the

Table 7. Comparison Between IRMS (with Reduce-Solve-Recombine Mechanism) and IRMS″ (Without Reduce-Solve-Combine Mechanism) on Synthetic and Real-World Benchmarks Under $\hat{t} = 3,600$ Seconds

			IRMS″			IRMS		
Instance	K	BKV	$\hat{f}$	$\bar{f}$	$\bar{t}$	$\hat{f}$	$\bar{f}$	$\bar{t}$
BA500	50	195*	**195**	**195.0**	0.0	**195**	**195.0**	0.0
BA1000	75	558*	**558**	**558.0**	0.5	**558**	**558.0**	3.1
BA2500	100	3,704*	**3,704**	**3,704.0**	2.7	**3,704**	**3,704.0**	3.9
BA5000	150	10,196*	**10,196**	**10,196.0**	26.1	**10,196**	**10,196.0**	16.8
ER235	50	295	**295**	**295.0**	1.8	**295**	**295.0**	6.5
ER466	80	1,524	**1,524**	**1,524.0**	240.9	**1,524**	**1,524.0**	83.7
ER941	140	5,012	**5,012**	5,076.0	1,929.7	**5,012**	5,020.0	520.0
ER2344	200	902,498	965,168	991,942.3	2,190.0	**920,748**	**944,406.9**	3,146.7
FF250	50	194*	**194**	**194.0**	0.1	**194**	**194.0**	0.0
FF500	110	257*	**257**	**257.0**	0.6	**257**	**257.0**	1.4
FF1000	150	1,260*	**1,260**	**1,260.0**	24.3	**1,260**	**1,260.0**	22.2
FF2000	200	4,545*	**4,545**	**4,545.0**	388.4	**4,545**	**4,545.0**	207.3

Table 7. (Continued)

			IRMS″			IRMS		
Instance	K	BKV	$\hat{f}$	$\bar{f}$	$\bar{t}$	$\hat{f}$	$\bar{f}$	$\bar{t}$
WS250	70	3,083	3,090	3,275.8	1,678.5	**3,085**	**3,179.0**	2,013.2
WS500	125	2,072	**2,072**	2,080.9	1,769.3	**2,072**	**2,080.1**	297.7
WS1000	200	109,677	141,667	146,811.2	2,039.8	**138,098**	**145,969.1**	1,963.2
WS1500	265	13,098	13,858	14,144.3	1,888.9	**13,098**	**13,112.9**	2,028.7
Bovine	3	268	**268**	**268.0**	0.0	**268**	**268.0**	0.0
Circuit	25	2,099	**2,099**	**2,099.0**	0.5	**2,099**	**2,099.0**	1.3
Ecoli	15	806	**806**	**806.0**	0.0	**806**	**806.0**	0.4
USAir97	33	4,336	**4,336**	4,674.0	314.4	**4,336**	**4,648.0**	668.8
HumanDi	52	1,115	**1,115**	**1,115.0**	0.3	**1,115**	**1,115.0**	0.1
TreniR	26	918	**918**	**918.0**	0.4	**918**	**918.0**	2.5
EU_fli	119	34,	**348,268**	348,350.8	1,705.8	**348,268**	**348,295.7**	998.0
openfli	186	26,783	29,118	29,497.6	2,059.9	**27,198**	**28,757.5**	1,695.8
yeast1	202	1,412	**1,412**	**1,412.0**	52.7	**1,412**	**1,412.0**	37.8
H1000	100	306,349	312,592	316,868.3	2,392.4	**306,349**	**308,951.9**	2,165.2
H2000	200	1,242,739	1,283,398	1,303,858.8	2,059.1	**1,236,503**	**1,254,481.6**	3,028.8
H3000a	300	2,840,690	2,909,699	2,961,854.3	1,670.9	**2,804,579**	**2,849,985.8**	3,088.5
H3000b	300	2,837,584	2,927,637	2,959,051.0	1,520.3	**2,801,186**	**2,842,174.8**	3,164.3
H3000c	300	2,835,369	2,906,920	2,948,294.3	2,130.8	**2,801,692**	**2,840,618.6**	3,066.0
H3000d	300	2,828,492	2,935,313	2,965,419.8	2,146.9	**2,816,590**	**2,864,256.5**	2,940.0
H3000e	300	2,843,000	2,927,917	2,964,465.5	2,202.5	**2,836,177**	**2,877,807.4**	2,715.4
H4000	400	5,038,611	5,246,420	5,317,627.6	1,881.6	**5,021,551**	**5,110,687.5**	3,042.0
H5000	500	7,964,765	8,289,948	8,388,331.1	1,929.4	**8,029,837**	**8,188,900.3**	2,741.0
powergr	494	15,862	15,938	15,990.4	2,692.5	**15,866**	**15,886.6**	3,021.6
Oclinks	190	611,253	**614,467**	**614,467.1**	1,402.9	**614,467**	614,467.6	1,038.9
facebook	404	420,334	755,714	805,713.6	1,894.0	**719,722**	**741,314.4**	2,852.1
grqc	524	13,591	13,635	13,652.6	2,764.6	**13,594**	**13,613.0**	3,201.9
hepth	988	106,276	126,106	137,745.1	1,652.7	**115,133**	**119,766.8**	3,159.4
hepph	1,201	6,155,877	10,255,932	11,239,245.2	2,946.7	**9,401,029**	**9,781,789.8**	3,077.4
astroph	1,877	53,963,375	62,169,348	63,174,914.0	2,410.7	**57,592,461**	**58,649,781.0**	3,271.4
condmat	2,313	2,298,596	9,943,424	10,804,865.5	2,416.2	**9,670,268**	**10,789,125.6**	2,286.2
No. of wins|ties|loses	–	–	21|21|0	25|16|1	–	–	–	–

Notes. The best values are highlighted in bold. * presents the optimal solution.

state-of-the-art heuristic algorithms, by discovering nine new upper bounds. Investigations are also performed that identify the benefit of different search modules and techniques used by the IRMS algorithm. In addition, we report computational results that demonstrate a generalization of IRMS likewise outperforms the previous best algorithm for the node-weighted critical node problem. The updated upper bounds can be useful for future research.

As future work, several potential research directions can be pursued. First, it would be interesting to optimally solve the reduced instance by an exact solver instead of approximately solving by a heuristic solver in the reduce-solve-combine module. Second, the reduce-solve-combine mechanism being a general-purpose technique for the instance reduction, its generality can be further verified by combining it with other metaheuristics, such as large neighborhood search (Schaap et al. 2022) and path relinking (Wu et al. 2020). Third, it is worth adapting IRMS to solver other problem variants, such as the distance-based critical node problem (i.e., there is a cost associated to each pair of nodes in the residual graph; Salemi and Buchanan 2022, Zhou et al. 2023c) and connected critical node problem (Hosteins et al. 2022). Finally, this work could benefit exact algorithms. For instance, we can employ IRMS to generate a high-quality initial solution for a given instance, whose objective function value is used as a tight starting upper bound.

Acknowledgments

The authors thank the editors and anonymous referees for insightful comments and suggestions that significantly improved this paper.

Endnote

[1] For the facebook and condmat instances, the best-known values were reported in Aringhieri et al. (2016a, table 5), which were reached only by the ILS-N_1-FC algorithm of Aringhieri et al. (2016b).

References

Abbas K, Abbasi A, Shi D, Ling N, Yu L, Chen B, Cai S, Hasan Q (2021) Application of network link prediction in drug discovery. *BMC Bioinformatics* 22(1):187.

Addis B, Aringhieri R, Grosso A, Hosteins P (2016) Hybrid constructive heuristics for the critical node problem. *Ann. Oper. Res.* 238(1–2):637–649.

Aiex RM, Resende MG, Ribeiro CC (2007) TTT plots: A perl program to create time-to-target plots. *Optim. Lett.* 1(4):355–366.

Archetti C, Boland N, Speranza MG (2017) A matheuristic for the multivehicle inventory routing problem. *INFORMS J. Comput.* 29(3):377–387.

Aringhieri R, Grosso A, Hosteins P, Scatamacchia R (2016a) A general evolutionary framework for different classes of critical node problems. *Engrg. Appl. Artificial Intelligence* 55:128–145.

Aringhieri R, Grosso A, Hosteins P, Scatamacchia R (2016b) Local search metaheuristics for the critical node problem. *Networks* 67(3):209–221.

Arnold F, Santana Í, Sörensen K, Vidal T (2021) PILS: Exploring high-order neighborhoods by pattern mining and injection. *Pattern Recognition* 116:107957.

Arulselvan A, Commander CW, Elefteriadou L, Pardalos PM (2009) Detecting critical nodes in sparse graphs. *Comput. Oper. Res.* 36(7):2193–2200.

Baggio A, Carvalho M, Lodi A, Tramontani A (2021) Multilevel approaches for the critical node problem. *Oper. Res.* 69(2):486–508.

Blum C, Davidson PP, López-Ibáñez M, Lozano JA (2016) Construct, merge, solve & adapt A new general algorithm for combinatorial optimization. *Comput. Oper. Res.* 68:75–88.

Boschetti MA, Maniezzo V (2022) Matheuristics: Using mathematics for heuristic design. *4OR* 20(2):173–208.

Cai S, Su K, Sattar A (2011) Local search with edge weighting and configuration checking heuristics for minimum vertex cover. *Artificial Intelligence* 175(9–10):1672–1696.

Chen W, Jiang M, Jiang C, Zhang J (2020) Critical node detection problem for complex network in undirected weighted networks. *Phys. A* 538:122862.

Chen Y, Hao JK (2014) A "reduce and solve" approach for the multiple-choice multidimensional knapsack problem. *Eur. J. Oper. Res.* 239(2):313–322.

Cooper WL, Homem-de-Mello T (2007) Some decomposition methods for revenue management. *Transportation Sci.* 41(3):332–353.

Cordeau J, Gaudioso M, Laporte G, Moccia L (2006) A memetic heuristic for the generalized quadratic assignment problem. *INFORMS J. Comput.* 18(4):433–443.

de Holanda Maia MR, Plastino A, Penna PHV (2020) Minereduce: An approach based on data mining for problem size reduction. *Comput. Oper. Res.* 122:104995.

de San Lázaro IM, Sánchez-Oro J, Duarte A (2021) Finding critical nodes in networks using variable neighborhood search. Mladenovic N, Sleptchenko A, Sifaleras A, Omar M, eds. *Proc. Variable Neighborhood Search* (Springer International Publishing, Cham, Switzerland), 1–13.

Delgadillo FJD, Montiel O, Sepúlveda R (2016) Reducing the size of traveling salesman problems using vaccination by fuzzy selector. *Expert Systems Appl.* 49:20–30.

Demšar J (2006) Statistical comparisons of classifiers over multiple data sets. *J. Machine Learn. Res.* 7(1):1–30.

Di Summa M, Grosso A, Locatelli M (2012) Branch and cut algorithms for detecting critical nodes in undirected graphs. *Comput. Optim. Appl.* 53(3):649–680.

Doostmohammadian M, Rabiee HR, Khan UA (2020) Centrality-based epidemic control in complex social networks. *Soc. Networks Anal. Mining* 10(1):32.

Fu ZH, Hao JK (2015) Dynamic programming driven memetic search for the steiner tree problem with revenues, budget, and hop constraints. *INFORMS J. Comput.* 27(2):221–237.

Glover FW (1997) A template for scatter search and path relinking. Hao JK, Lutton E, Ronald EMA, Schoenauer M, Snyers D, eds. *Proc. AE* (Springer, Berlin), 1–51.

Grahne G, Zhu J (2005) Fast algorithms for frequent itemset mining using fp-trees. *IEEE Trans. Knowledge Data Engrg.* 17(10):1347–1362.

Hao JK, Wu Q (2012) Improving the extraction and expansion method for large graph coloring. *Discrete Appl. Math.* 160(16–17):2397–2407.

Hopcroft J, Tarjan R (1973) Algorithm 447: Efficient algorithms for graph manipulation. *Comm. ACM* 16(6):372–378.

Hosteins P, Scatamacchia R, Grosso A, Aringhieri R (2022) The connected critical node problem. *Theoretical Comput. Sci.* 923:235–255.

Kenny A, Li X, Ernst AT (2018) A merge search algorithm and its application to the constrained pit problem in mining. Aguirre HE, Takadama K, eds. *Proc. GECCO* (ACM, New York), 316–323.

Kenny A, Li X, Ernst AT, Sun Y (2019) An improved merge search algorithm for the constrained pit problem in open-pit mining. *Proc. GECCO* (ACM, New York), 294–302.

Le HL, Neri F, Triguero I (2022) SPMS-ALS: A single-point memetic structure with accelerated local search for instance reduction. *Swarm Evolution Comput.* 69:100991.

Luna JM, Fournier-Viger P, Ventura S (2019) Frequent itemset mining: A 25 years review. *Data Mining Knowledge Discovery* 9(6):e1329.

Mihic K, Ryan K, Wood A (2018) Randomized decomposition solver with the quadratic assignment problem as a case study. *INFORMS J. Comput.* 30(2):295–308.

Montiel O, Delgadillo FJD, Sepúlveda R (2013) Combinatorial complexity problem reduction by the use of artificial vaccines. *Expert Systems Appl.* 40(5):1871–1879.

Mugisha S, Zhou HJ (2016) Identifying optimal targets of network attack by belief propagation. *Phys. Rev. E* 94:012305.

Nabli A, Carvalho M (2020) Curriculum learning for multilevel budgeted combinatorial problems. *Adv. Neural Inform. Processing Systems* 33:7044–7056.

Naoum-Sawaya J, Buchheim C (2016) Robust critical node selection by benders decomposition. *INFORMS J. Comput.* 28(1):162–174.

Neri F, Cotta C (2012) Memetic algorithms and memetic computing optimization: A literature review. *Swarm Evolution Comput.* 2:1–14.

Nguyen DT, Shen Y, Thai MT (2013) Detecting critical nodes in interdependent power networks for vulnerability assessment. *IEEE Trans. Smart Grid* 4(1):151–159.

Plastino A, Barbalho H, Santos LFM, Fuchshuber R, Martins SL (2014) Adaptive and multi-mining versions of the DM-GRASP hybrid metaheuristic. *J. Heuristics* 20(1):39–74.

Pullan W (2015) Heuristic identification of critical nodes in sparse real-world graphs. *J. Heuristics* 21(5):577–598.

Purevsuren D, Cui G, Qu M, Win NH (2017) Hybridization of GRASP with exterior path relinking for identifying critical nodes in graphs. *IAENG Internat. J. Comput. Sci.* 44(2):157–165.

Rezaei J, Zare-Mirakabad F, MirHassani SA, Marashi S (2021) EIA-CNDP: An exact iterative algorithm for critical node detection problem. *Comput. Oper. Res.* 127:105138.

Ribeiro MH, Plastino A, Martins SL (2006) Hybridization of GRASP metaheuristic with data mining techniques. *J. Math. Modeling Algorithms* 5(1):23–41.

Salemi H, Buchanan A (2022) Solving the distance-based critical node problem. *INFORMS J. Comput.* 34(3):1309–1326.

Schaap H, Schiffer M, Schneider M, Walther G (2022) A large neighborhood search for the vehicle routing problem with multiple time windows. *Transportation Sci.* 56(5):1369–1392.

Subramanyam A, Gounaris CE (2018) A decomposition algorithm for the consistent traveling salesman problem with vehicle idling. *Transportation Sci.* 52(2):386–401.

Tarjan R (1972) Depth-first search and linear graph algorithms. *SIAM J. Sci. Comput.* 1(2):146–160.

Thornton J, Pham DN, Bain S, Ferreira V Jr (2004) Additive vs. multiplicative clause weighting for SAT. McGuinness DL, Ferguson G, eds. *Proc. AAAI*, 191–196.

Ventresca M (2012) Global search algorithms using a combinatorial unranking-based problem representation for the critical node detection problem. *Comput. Oper. Res.* 39(11):2763–2775.

Ventresca M, Aleman D (2014) A derandomized approximation algorithm for the critical node detection problem. *Comput. Oper. Res.* 43:261–270.

Ventresca M, Aleman D (2015) Efficiently identifying critical nodes in large complex networks. *Comput. Soc. Networks* 2(1):1–16.

Veremyev A, Boginski V, Pasiliao EL (2014a) Exact identification of critical nodes in sparse networks via new compact formulations. *Optim. Lett.* 8(4):1245–1259.

Veremyev A, Prokopyev OA, Pasiliao EL (2014b) An integer programming framework for critical elements detection in graphs. *J. Combinatorial Optim.* 28(1):233–273.

Veremyev A, Prokopyev OA, Pasiliao EL (2019) Finding critical links for closeness centrality. *INFORMS J. Comput.* 31(2):367–389.

Vitoriano B, Ortuño MT, Tirado G, Montero J (2011) A multi-criteria optimization model for humanitarian aid distribution. *J. Global Optim.* 51(2):189–208.

Wang Z, Di Y (2022) Cluster expansion method for critical node problem based on contraction mechanism in sparse graphs. *IEICE Trans. Inform. Systems* 105-D(6):1135–1149.

Wu Q, Hao JK (2012) Coloring large graphs based on independent set extraction. *Comput. Oper. Res.* 39(2):283–290.

Wu Q, Hao JK (2013) An extraction and expansion approach for graph coloring. *Asia-Pacific J. Oper. Res.* 30(5):1350018.

Wu Q, Wang Y, Glover F (2020) Advanced tabu search algorithms for bipartite boolean quadratic programs guided by strategic oscillation and path relinking. *INFORMS J. Comput.* 32(1):74–89.

Zhang Y, Mei Y, Zhang B, Jiang K (2021) Divide-and-conquer large scale capacitated arc routing problems with route cutting off decomposition. *Inform. Sci.* 553:208–224.

Zhang Y, Chen Q, Chen B, Liu J, Zheng H, Yao H, Zhang C (2020) Identifying hotspots of sectors and supply chain paths for electricity conservation in china. *J. Clean Production* 251:119653.

Zheng Y, Xue J (2010) A problem reduction based approach to discrete optimization algorithm design. *Computing* 88(1):31–54.

Zhou Y, Hao JK, Duval B (2022) Frequent pattern-based search: A case study on the quadratic assignment problem. *IEEE Trans. Systems Man Cybernics Systems* 52(3):1503–1515.

Zhou Y, Hao JK, Glover F (2019) Memetic search for identifying critical nodes in sparse graphs. *IEEE Trans. Cybernetics* 49(10):3699–3712.

Zhou Y, Kou Y, Zhou M (2023a) Bilevel memetic search approach to the soft-clustered vehicle routing problem. *Transportation Sci.* 57(3):701–716.

Zhou Y, Li J, Hao JK, Glover F (2023b) Detecting critical nodes in sparse graphs via "reduce-solve-combine" memetic search. http://dx.doi.org/10.1287/ijoc.2022.0130.cd, https://github.com/INFORMSJoC/2022.0130.

Zhou Y, Wang Z, Jin Y, Fu ZH (2021a) Late acceptance-based heuristic algorithms for identifying critical nodes of weighted graphs. *Knowledge Base. Systems* 211:106562.

Zhou Y, Hao JK, Fu ZH, Wang Z, Lai X (2021b) Variable population memetic search: A case study on the critical node problem. *IEEE Trans. Evolution Comput.* 25(1):187–200.

Zhou Y, Kundu T, Qin W, Goh M, Sheu JB (2021c) Vulnerability of the worldwide air transportation network to global catastrophes such as covid-19. *Transportation Res. Part E Logist. Transportation Rev.* 154:102469.

Zhou Y, Wang G, Hao JK, Geng N, Jiang Z (2023c) A fast tri-individual memetic search approach for the distance-based critical node problem. *Eur. J. Oper. Res.* 308(2):540–554.

Zhou Y, Zhang X, Geng N, Jiang Z, Wang S, Zhou M (2023d) Frequent itemset-driven search for finding minimal node separators and its application to air transportation network analysis. *IEEE Trans. Intelligent Transportation Systems* 24(8):8348–8360.